AFRL-RQ-ED-TR-2017-0025

Non-Toxic Multifunctional Silsesquioxane Diamine Monomer for Use in Aerospace Polyimides

Gregory Yandek

Air Force Research Laboratory (AFMC)
AFRL/RQRP
Propellants Branch
10 E. Saturn Blvd.
Edwards AFB, CA 93524

November 2017

In-House SERDP WP-2403 Final Report

AIR FORCE RESEARCH LABORATORY
AEROSPACE SYSTEMS DIRECTORATE

■ Air Force Materiel Command ■ United States Air Force ■ Edwards Air Force Base, CA 93524

- STINFO COPY -
NOTICE AND SIGNATURE PAGE

Using Government drawings, specifications, or other data included in this document for any purpose other than Government procurement does not in any way obligate the U.S. Government. The fact that the Government formulated or supplied the drawings, specifications, or other data does not license the holder or any other person or corporation; or convey any rights or permission to manufacture, use, or sell any patented invention that may relate to them.

This report was cleared for public release by the USAF 412 Test Wing (412 TW) Public Affairs Office (PAO) and is available to the general public, including foreign nationals.

AFRL-RQ-ED-TR-2017-0025 HAS BEEN REVIEWED AND IS APPROVED FOR PUBLICATION IN ACCORDANCE WITH ASSIGNED DISTRIBUTION STATEMENT.

FOR THE DIRECTOR:

//Signature//

GREGORY R. YANDEK, Ph.D.
Program Manager

//Signature//

ANDREW J. GUENTHNER, Ph.D.
Technical Advisor, Propellants Branch

//Signature//

Technical Advisor
Rocket Propulsion Division

This report is published in the interest of scientific and technical information exchange, and its publication does not constitute the Government's approval or disapproval of its ideas or findings.

REPORT DOCUMENTATION PAGE

Form Approved
OMB No. 0704-0188

1. REPORT DATE *(MM/DD/YYYY)*	**2. REPORT TYPE**	**3. DATES COVERED** *(From - To)*
11/3/2017	SERDP WP-2403 Final Report	1/06/2014 – 7/10/2015

4. TITLE AND SUBTITLE
Non-Toxic Multifunctional Silsesquioxane Diamine Monomer for Use in Aerospace Polyimides

5a. CONTRACT NUMBER
In-House

5b. GRANT NUMBER

5c. PROGRAM ELEMENT NUMBER

6. AUTHOR(S)
Gregory Yandek

5d. PROJECT NUMBER
SERDP WP-2403

5e. TASK NUMBER

5f. WORK UNIT NUMBER
Q16J

7. PERFORMING ORGANIZATION NAME(S) AND ADDRESS(ES)

Air Force Research Laboratory (AFMC)
AFRL/RQRP
10 E. Saturn Blvd.
Edwards AFB, CA 93524

8. PERFORMING ORGANIZATION REPORT NO.
AFRL-RQ-ED-TR-2017-0025

9. SPONSORING / MONITORING AGENCY NAME(S) AND ADDRESS(ES)

Strategic Environmental Research and Development Program (SERDP)
4800 Mark Center Drive
Suite 17D03
Alexandria, VA 22350-3605

10. SPONSOR/MONITOR'S ACRONYM(S)

11. SPONSOR/MONITOR'S REPORT NUMBER(S)

12. DISTRIBUTION / AVAILABILITY STATEMENT
Approved for public release; distribution unlimited.

13. SUPPLEMENTARY NOTES
PA Clearance No. 17761; SERDP Final Report WP-2403

14. ABSTRACT

The effectiveness of an experimental, non-commercial diamine monomer as a replacement for methylene dianiline (MDA) in the commercial polyimide PMR-15, was assessed in this SERDP research project. The monomer, designed and synthesized at AFRL, features a polyhedral oligomeric silsesquioxane (POSS) core with an aromatic periphery to maximize its thermal stability. MDA is a known irritant, causative agent for liver damage, and possible carcinogen to humans as it has been found to cause liver and thyroid cancer in mice. In response, OSHA has set a low permissible exposure limit and replacement efforts for materials containing MDA are ongoing. Unfortunately, many efforts spanning approximately 35 years seeking an alternative to MDA in PMR-15 have not produced a solution that affords an equivalent balance of properties. The POSS monomer was chosen based on speculation of non-toxicity based on its chemical structure and high molecular weight. Furthermore, premise for this work was in part because of the novelty of POSS and its chemical framework for this particular application. Due to the limited scope of this SEED project, the POSS diamine was not examined for any biological effects but could be the focus of future studies. The subject POSS monomer was used as a drop-in replacement for MDA in heritage PMR-15 chemistry and resultant oligoimide, cured polyimide, and carbon fiber reinforced composite properties were examined.

15. SUBJECT TERMS
PMR-15 replacement, methylene dianiline, high temperature polymer matrix composites, polyhedral oligomeric silsesquioxane, POSS, polyimide, micro-cracking

16. SECURITY CLASSIFICATION OF:			**17. LIMITATION OF ABSTRACT**	**18. NUMBER OF PAGES**	**19a. NAME OF RESPONSIBLE PERSON**
					Dr. Gregory Yandek
a. REPORT	**b. ABSTRACT**	**c. THIS PAGE**			**19b. TELEPHONE NO** *(include area code)*
Unclassified	**Unclassified**	**Unclassified**	SAR	65	661 277-7192

Standard Form 298 (Rev. 8-98)
Prescribed by ANSI Std. 239.18

This Page Intentionally Left Blank

Table of Contents

List of Figures

List of Tables

List of Acronyms

6-FDA:	4,4′-(Hexafluoro-isopropylidiene)diphthalic Anhydride
AFB:	Air Force Base
AFR-PE	Air Force Resin-Phenylethynyl
AFRL:	Air Force Research Laboratory
ASTM:	American Society for Testing and Materials
BAPP:	2,2′-Bis[4-(4-aminophenoxy)phenyl]propane
BTDA:	3,3′,4,4′-benzophenonetetracarboxylic dianhydride
BTDE:	3,3′,4,4′-Benzophenonetetracarboxylic Diester
BMI:	Bismaleimide
CTC:	Charge Transfer Complexing
CTE	Coefficient of Thermal Expansion
CYP:	Cytochrome P450
DMA:	Dynamic Mechanical Analysis
DMBZ:	2,2′-Dimethylbenzidine
DoD:	Department of Defense
DSC:	Differential Scanning Calorimetry/Calorimeter
EPA:	Environmental Protection Agency
ESOH:	Environmental, Safety, and Occupational Health
FTIR:	Fourier Transform Infrared Spectroscopy
HSW:	Harness Satin Weave
HTS:	High Temperature Sizing
ILSS:	Interlaminar Shear Strength
IM:	Intermediate Modulus
KOH:	Potassium Hydroxide
L/h:	Span/Thickness
MDA:	4,4’-Methylenedianiline
MeOH:	Methanol
Mn:	number average molecular weight of a polymer
NASA:	National Aeronautics and Space Administration
NA:	Nadic Anhydride
NE:	5-Norbornene-2,3′-dicarboxylic Half Acid Ester
NMR:	Nuclear Magnetic Resonance Spectroscopy
ODA:	3,4′,4,4′-Oxydianiline
OMC:	Organic Matrix Composite
PA:	Phthalic Anhydride
PE:	Phenylethynyl
PEPA:	Phenylethynyl Phthalic Anhydride
PMDA:	pyromellitic dianhydride
p-PDA:	p-Phenylenediamine
POSS:	Polyhedral Oligomeric Silsesquioxane
PMR:	Polymerizable Monomeric Reactants
RP-21:	Rocket Propulsion 21
RTM:	Resin Transfer Molding
SEED:	SERDP Exploratory Development

SERDP:	Strategic Environmental Research and Development Program
SiO_2:	Silicon Dioxide
T_g:	Glass Transition Temperature
TGA:	Thermogravimetric Analysis
TMA:	Thermomechanical Analysis
TOS:	Thermo-Oxidative Stability
TRL:	Technology Readiness Level

Keywords

PMR-15 replacement, methylene dianiline, high temperature polymer matrix composites, polyhedral oligomeric silsesquioxane, POSS, polyimide, micro-cracking

Acknowledgements

The authors gratefully thank the Strategic Environmental Research and Development Program (SERDP) Weapons and Platforms Office, under the leadership of Dr. Robin Nissan, for the funded opportunity to perform the research presented herein. The key performers on this challenging project were instrumental in making the effort a success, including: Mr. Jason T. Lamb (ERC, Inc. - synthesis, fabrication, and characterization), Dr. Timothy S. Haddad (ERC, Inc. - synthesis guidance and NMR analysis expertise), Dr. Joseph M. Mabry (AFRL – synthesis guidance), Lt. Diane Fernandes (AF – POSS dianiline synthesis), Mr. Michael Ford (ERC, Inc. - NMR characterization and analysis), and Dr. Andrew J. Guenthner (AFRL – structure-property relationships). Without their skills and expertise the breadth of results learned from this project would not have been possible. Discussions with Dr. Thomas Tsotsis (Boeing Phantom Works) and Mr. Robert Gray (Maverick Composites) on commercialization opportunities and pathways were also extremely guiding and beneficial, as well as technical discussions with Prof. Andre Lee (Michigan State University – Department of Chemical Engineering and Materials Science). We also thank Ms. Sara Betz, Ms. Jo ann La Rue, and Ms. Amanda Wheaton for administrative assistance during this effort.

This Page Intentionally Left Blank

Abstract

Objectives

The effectiveness of an experimental, non-commercial diamine monomer as a replacement for methylene dianiline (MDA) in the commercial polyimide PMR-15, was assessed in this SERDP research project. The monomer, designed and synthesized at AFRL, features a polyhedral oligomeric silsesquioxane (POSS) core with an aromatic periphery to maximize its thermal stability. MDA is a known irritant, causative agent for liver damage, and possible carcinogen to humans as it has been found to cause liver and thyroid cancer in mice. In response, OSHA has set a low permissible exposure limit and replacement efforts for materials containing MDA are ongoing. Unfortunately, many efforts spanning approximately 35 years seeking an alternative to MDA in PMR-15 have not produced a solution that affords an equivalent balance of properties. The POSS monomer was chosen based on speculation of non-toxicity based on its chemical structure and high molecular weight. Furthermore, premise for this work was in part because of the novelty of POSS and its chemical framework for this particular application. Due to the limited scope of this SEED project, the POSS diamine was not examined for any biological effects but could be the focus of future studies. The subject POSS monomer was used as a drop-in replacement for MDA in heritage PMR-15 chemistry and resultant oligoimide, cured polyimide, and carbon fiber reinforced composite properties were examined.

Technical Approach

Two strategies were explored to synthesize different families of oligomers containing the POSS diamine. In a more conventional approach, the POSS diamine was reacted with three ratios of the dianhydride monomers utilized in PMR-15, namely 3,3′,4,4′-benzophenonetetracarboxylic dianhydride (BTDA) and nadic anhydride (NA), to render oligomers of variant average molecular weight and POSS content. In the second approach, pursued as a parallel path for the sole purpose of risk reduction, the POSS dianiline was reacted with phthalic anhydride (PA), p-phenylene dianiline (p-PDA), and NA endcap. Oligomerization of PA and p-PDA is known to render an intractable material. However, impetus for this approach was the expectation that PA and p-PDA may result in a material with very high thermal stability, and POSS typically imparts improved processing characteristics manifested in lower viscosity.

Oligomers were characterized in screening studies for their uncured and cured properties, and compared with PMR-15. The properties that were selected for comparison were chosen based on their criticality to processing and performance, including flow viscosity, post-cure glass transition temperature, moisture diffusion and saturated weight content, and short and long-term thermal stability. In general, properties quantified to be within 5% of those of PMR-15 based on literature values, when available, or from direct comparison of measured values, met a threshold for viability. The candidate featuring the highest glass transition temperature was selected for a synthesis reaction at a suitable scale to facilitate composite fabrication. Resultant composite laminates were sectioned and characterized mechanically for interlaminar and flexural strength properties, chosen for examination because of risk identification as these are resin dominated properties. Interlaminar shear strength is an indicator of the adhesion between fabric and resin,

while the flexural strength is affected by resin toughness. Composites were also tested for their long-term thermo-oxidative stability (TOS) and micro-cracking behavior.

Results

PMR-15 oligomers are commercially synthesized in methanol via anhydride esterification, and the resultant solution is utilized to impregnate (pre-preg) textile tapes and fabrics. It was found that the subject POSS monomer is insoluble in methanol, unlike MDA. All synthesis reactions involving POSS were therefore conducted in tetrahydrofuran (THF), and conversations with the pre-pregging industry revealed that this solvent could be used in manufacturing as it is considered relatively nontoxic.

Pure substitution of MDA with POSS in heritage PMR-15 chemistry ($BTDA_2$-$POSS_3$-NA_2) produced mixed results. Fortuitously, integrity of the POSS cage was confirmed by nuclear magnetic resonance (NMR) spectroscopy after synthesis and amic acid imidization. POSS was found to improve the processing characteristics by reducing flow viscosity above the glass transition temperature, but also reduced the cured glass transition temperature by 77 °C. The long-term thermo-oxidative stability at 316 °C was not affected, behaving equivalently to PMR-15, up to almost 700 hours. Saturated moisture uptake in boiling water was lessened by 80%.

The negative impact of POSS oligomerization on cured glass transition temperature is due to its large molecular dimensions, and probably to a lesser extent, the ability for the POSS cage to relax under mechanical or thermal stimuli (the cage is not rigid but somewhat flexible). Consequently, POSS segments yield oligomers of greater length and volumetric footprint than PMR-15, and in the cured state, the distance between crosslink junctions must be greater. In attempts to offset this, two shortened oligomers in a series were synthesized, one less a repeat unit ($BTDA_1$-$POSS_2$-NA_2), and another devoid of BTDA ($POSS_1$-NA_2). Although the cured glass transition temperature increased with decreasing average oligomer length, the thermo-oxidative stability suffered, and this was presented to be due to the higher concentrations of the nadic group, and its cross-linked products. Nonetheless, the $POSS_1$-NA_2 oligomer was selected for composite fabrication and testing because it demonstrated the highest cured glass transition temperature of the series. The alternative strategy to oligomerize POSS with PA, p-PDA, and NA resulted in intractable and insoluble materials for the stoichiometries examined.

A 200 gram batch of $POSS_1$-NA_2 was synthesized and pre-pregged using Hexcel IM7 four harness satin weave fabric. A composite laminate panel was fabricated, sectioned, and tested for interlaminar shear strength, flexural properties, and long-term thermo-oxidative stability. All properties were measured to be significantly less than those of PMR-15 composite: short beam shear, -71%, flexural strength, -78%, and TOS, 3.1% weight loss vs. 0.7% for PMR-15 composite after 625 hours at 316 °C. One significantly positive finding is that the $POSS_1$-NA_2 exhibited no micro-crack initiation and growth during long-term TOS, as opposed to PMR-15.

Benefits

The POSS dianiline examined in this effort improves resin processability and moisture resistance, and prevents aging induced micro-cracking at elevated temperature, is sufficiently thermally stable to be utilized in high performance polyimide chemistries, but reduces cured glass transition temperature. This reduction was offset by shortening average oligomer chain length, but resin dominated mechanical properties such as those quantified herein suffered as a result.

Although weight loss during elevated temperature aging in air was accelerated for some of the experimental oligomers, this result was traced to nadic end group concentration rather than the POSS monomer itself. Implications for structure manufacturing are that POSS could facilitate the fabrication of composite parts using high temperature capable oligomers by resin transfer molding (RTM), where the textile preform is infiltrated with resin via a simple flow process, only possible with resin systems of sufficiently low viscosity. Currently, RTM is viable with lower performing resin systems such as epoxies and BMIs, but not many polyimides. The RTM method is gaining momentum in industry as it does not require solvent and is simpler in practice, therefore there is a growing need for high temperature capable, low flow viscosity resin systems. In service, POSS containing composite materials are expected to have enhanced survivability, especially in hot-wet conditions and due to their observed resistance to micro-cracking.

The observation of lower cured glass transition temperatures with POSS utilization requires additional oligomer design to maximize the effectiveness of its implementation, and should be the subject of future studies to enhance technological viability. Use of an alternative crosslinking group was superficially studied as part of this effort, namely phenylethynyl phthalic anhydride (PEPA), well known to afford higher cured glass transition temperature and thermal stability than nadic anhydride. Initial results are promising, thus deserving of further focus. The results produced from this effort have been presented to the DoD, NASA, relevant industry firms, and academia at several conferences including ACS, High Temple, and SAMPE. The general response is that the observations of moisture uptake resistance, but most noteworthy the elimination of micro-cracking induced by thermo-oxidative aging, at least within the conditions implemented in this study, provide hope that the issues that have long plagued composite materials might one day be overcome.

During the design phase of aerospace components, the use of organic matrix composites is often precluded due to their current service life, but POSS could provide a solution to extending this attribute thereby expanding their utility in reducing the weight of systems in a sustainable manner. The manufacturing shift towards RTM due to its simplicity, speed, and reliability is expected to increase in intensity, but the implementation of high temperature resin systems in this process is thus far impossible due to their intrinsically high viscosities. The incorporation of POSS into the backbone of thermosetting oligomides reduces viscosity to an extent that it could be possible to use resin systems conventionally disregarded for RTM processing without compromising their thermal stability. To promote adoption of this technology by industry, future work should therefore focus on detailing the amount of POSS monomer needed in a high temperature matrix resin to eliminate micro-cracking in concert with developing an oligomeric architecture that is amenable to RTM processing. The coupling of these two attributes with high temperature capability and non-toxic character would provide a revolutionary yet sustainable organic composite material technology available for the manufacture of next-generation aerospace systems.

Objective

The overall research objectives for this project were to determine if an experimental polyhedral oligomeric silsesquioxane (POSS) diamine is a suitable drop-in replacement for MDA in PMR-type resin systems, and if the diamine could be used to develop alternative high performance resin chemistries to PMR-15. MDA is a known toxin, thus motivating replacement efforts and the solicitation under which this project was funded. The POSS diamine is suspected of being biologically non-toxic due to its molecular size and chemical makeup. Preliminary in-house studies prior to this SERDP project showed that the POSS dianiline monomer could be readily oligomerized with a few standard PMR-type monomers, but its feasibility in the PMR-15 chemical framework had not been examined. Basic characterization efforts on uncured and cured oligomers demonstrated that the use of the subject monomer provides, in many cases, superior properties to a dianiline monomer similar in structure to MDA, namely 4,4′-oxydianiline (ODA).

For this project, monomer viability was further assessed through the synthesis of oligomers adopting the subject monomer, which were subjected to screening studies for key properties and compared to those of heritage PMR-15. The key properties chosen for comparison with PMR-15 were selected based on the most basic expectations for resin systems used to fabricate fiber reinforced organic matrix composites for service in aerospace applications. The most promising candidate was selected for larger scale synthesis from which carbon fiber fabric pre-preg was made ultimately resulting in cured laminate panels. These laminates were sectioned and tested for key properties.

This project addressed the following key questions: 1) could the subject POSS monomer be oligomerized using the PMR-15 chemical framework as a replacement for MDA, as well as in other PMR-type resin systems; 2) are the properties of this new class of resins equivalent or superior to those of PMR-15; and 3) are the properties of fiber-reinforced composites fabricated from the new class of resins equivalent or superior to those based on PMR-15. The work plan consisted of chemical synthesis, test article fabrication, and material property characterization activities. Synthesis activities ascertained the reactivity of the silsesquioxane monomer with other monomers of interest. Oligomer analyses included imidization and curing kinetics, as well as processability evaluations. Cured polyimide characterization entailed measurement of viscoelastic properties including glass transition temperatures (T_g), thermo-oxidative stability (TOS), moisture diffusion and saturated content, and select resin-dominated mechanical properties. All properties were compared to those of control specimens which were fabricated in-house using similar procedures from PMR-15 resin synthesized in our laboratory. This comparison of properties along with those extracted from literature sources for PMR-15 were used as the basis for an assessment of the viability of replacing MDA with the silsesquioxane monomer. The results yielded from this SEED project could be utilized as the basis for future oligomer design, synthesis, and characterization efforts, including toxicology studies on the POSS dianiline, followed by aerospace component manufacturing demonstrations and testing in relevant environments, in preparation for the technology transition of the technology to industry.

Background

PMR-15, developed by NASA Lewis Research Center in the 1970s, is the aerospace industry's most prolifically utilized high temperature OMC matrix resin for lightweight hot structures in aircraft and other applications because it offers ease of processing and good property retention in service at reasonable cost [1-4]. The most prolific consumption of PMR-15 is in the production of GE Aviation's F/A-18E/F & EA-18G engines, where the F414 Outer Bypass Duct is comprised of PMR-15 composite. Although annual consumption is variable, it is estimated that on average over 20,000 lbs of PMR-15 are consumed per year, the vast majority of which is utilized for DoD subsidized aircraft production programs [5]. The popularity of PMR-15 is based on its unique combination of properties, including processability, service temperature (max 288 °C), long-term TOS, and mechanical properties including fracture toughness and resistance to micro-cracking. However, since the early 1980s, it has been recognized that MDA, a key monomer in PMR-15, poses health risks and therefore has been under intense ESOH scrutiny. In the state of California, for example, Lockheed Martin Skunk Works has eliminated the use of PMR-15 in aircraft design activities due to state restrictions on material handling and ESOH practices. While material solutions are available for lower service temperatures (BMIs) as well as for higher service temperatures (AFR-PE), materials for mid-service temperatures, like PMR-15, are notably deficient. Therefore, the health effects of MDA are currently affecting design on DoD acquisition programs and a solution to fill this gap is needed.

The dangers associated with MDA ingestion have been studied and are well understood. In the human body, the cytochrome P450 (CYP) class of enzyme is used to oxidize organic chemicals in the body and liver [6-7]. However, CYP bioactivates MDA and its derivatives to form nitroso compounds, via N-oxidation, that can then be converted to nitrosamines, a class of compounds known to be highly toxic [8-9]. Additionally, the reactive intermediates can form an elimination product that conjugates with glutathione, thereby depleting the concentration of this oxygen free radical scavenger that protects against DNA degradation, which can cause cancer [10-12]. As a consequence, the life cycle costs associated with PMR-15 have increased due to required handling measures to mitigate its health risks to humans and the environment. Furthermore, the supply chain of MDA to oligoimide pre-preggers, cascading to U.S. aerospace manufacturers, has been disrupted due to the limited number of producers of the monomer, which are all in Asia. In fact, the U.S. now procures MDA from only one Japanese source because the remaining manufacturers are based in China. Because of these circumstances, research and development efforts focused on alternative resin systems to replace PMR-15 have been numerous since the early 1980s. Despite the successes of many of these efforts, including the commercialization of a limited number of oligoimides developed by NASA, alternative chemistries exhibiting equivalent properties and cost have remained elusive. Of the over 50 known reported diamines studied as alternatives to MDA, including those possessing phenyl linkage groups such as ketone, sulfur, sulfone, ether, unsaturated aliphatic groups, as well as three and four-phenyl ring diamines, none have afforded the combination of T_g, >1000 hr weight loss at 288 °C, and mechanical properties that the use of MDA provides [13]. A few notable examples which have been commercialized are AMB-21, employing 2,2′-bis[4-(4-aminophenoxy)phenyl]propane (BAPP), and LARC-RP-26, employing 3,4′-oxydianiline (ODA), feature enhanced processability, but 75 and 65 °C lower T_gs than PMR-15, respectively. Monomers imparting higher T_gs than MDA such as NASA's developed asymmetric class of monomers, most notably 2,2′-dimethylbenzidine (DMBZ), also

recently commercialized in PMR chemistry, suffer from lower long-term TOS due to their methyl groups.

PMR-15 chemistry involves the polymerization of the following monomers: MDA, 5-norbornene-2,3′-dicarboxylic half acid ester (NE), and 3,3′,4,4′-benzophenonetetracarboxylic diester (BTDE), as shown in Figure 1. The MDA monomer, possessing a single methylene bridge between two aniline groups, is uniquely effective due to its balance between thermal stability (low aliphatic character) and slight flexibility thus imparting a certain degree of processability to oligomers. Therefore, as described in the preceding paragraph, the task of replacing MDA, while retaining its most useful properties, has proven to be considerably challenging. **In stark contrast to all known documented approaches to the search for safer MDA alternatives, our approach consists of utilizing a silsesquioxane-based dianiline monomer featuring a silicon-oxygen core and aromatic, thermally stable organic periphery** [14]. The core compound that is used to synthesize this dianiline, a polyhedral oligomeric silsesquioxane (POSS) tetrasilanol, is manufactured by a U.S.-based company (Hybrid Plastics, Hattiesburg, MS). Although the toxicity of the subject diamine has not been specifically studied, it is not expected to present toxicity issues due to its relatively high molecular weight and chemical architecture. Several published works have investigated the toxicity of POSS compounds in biological systems [15-20]. Non-reactive versions of POSS have been shown to be non-toxic in oral ingestion tests in rats. Most relevant to this proposal, Rotello et al demonstrated that amine functionalized POSS molecules exhibit very low toxicity to Cos-1 cells derived from monkey kidney tissue, as evidenced by cell vitality after POSS incubation [15]. POSS-containing copolymers have also been investigated for their biocompatibility and functionality for cardiovascular device applications [17-18, 20], other biomedical devices [19], and recently as a molecular scaffold to engineer tissue replacements for human noses [21]. Based on these studies and the growing interest in POSS for biomedical applications, we believe that POSS will serve as a safe alternative to MDA in PMR-type systems. Not only can the subject POSS diamine improve the ESOH characteristics of PMR resins, but it is expected to provide equivalent delivered properties to PMR-15 in many areas, and impart even superior properties in others.

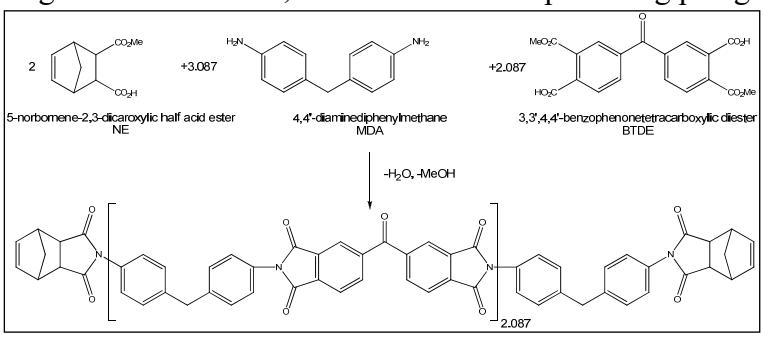

Figure 1. Chemical structures and general reaction scheme to oligomerize PMR-15.

To summarize our work using the subject POSS dianiline prior to this project, the monomer, shown in Figure 2, had been copolymerized with 4,4′-(hexafluoro-isopropylidiene)diphthalic anhydride (6-FDA), 4,4′-oxydianiline (ODA), and phenylethynyl phthalic anhydride (PEPA) endcap, monomers common to PMR chemistries, to produce short chain cross-linkable oligoimides of n_{ave}=4 [22]. These monomers and generalized synthesis strategy are also shown in Figure 2. It should be noted that ODA is considered to be a carcinogen and it also tends to lower post-cured T_g, so this research study represents merely a proof of concept rather than development of a feasible commercial product. The POSS content was systematically altered to yield oligomers possessing no POSS (control) to 3 POSS units on average. Consequently, ODA content also varied. Target molecular weights were achieved and the POSS

cage remained intact during oligomer synthesis. The oligomers were cured using standard heat and pressure protocol prescribed for phenylethynyl (PE) crosslinking to yield neat resin specimens. Characterization of this suite of polyimides revealed very promising properties First, co-oligomerization with POSS reduces zero shear viscosity by an order of magnitude, thus improving processing characteristics and opening up the possibility of processing polyimide composites by unconventional means. Despite the size of the POSS monomer in relation to the other involved constituents, the post-cured T_g of the polyimide possessing the highest POSS content was only 30 °C lower than that of the control (290 °C vs. 320 °C). A knockdown is to be expected if the oligomer repeat units are kept constant, due to the greater length of the POSS segment in relation to ODA. Greater segment length between crosslinks is known to reduce T_g. This reduction will be countered by controlling segment length in this effort. The thermal stabilities of the POSS-polyimides were measured to be nearly identical to that of the control in an inert atmosphere (nitrogen), but improved in air. This is due to the oxidation of POSS to form a protective silicon dioxide (SiO_2) layer, analogous to our work which studied POSS-polyimides in low earth orbit, where degradative atomic oxygen is present [23]. Organic Matrix Composites (OMCs) are known to degrade by oxidation in long term elevated air temperature experiments both from the edges of the structure inward as well as along the fiber-polymer matrix interphase outward. This oxidation obviously reduces delivered properties. The prevalence of POSS in the polymer matrix is expected to efficiently serve to protect OMCs from oxidative aging by forming a protective layer of SiO_2 at the air-polymer interface. Unlike coating technologies, this layer can be generated and regenerated if micro-cracks form as a result of thermal cycling or if it is damaged. Finally, copolymerization with POSS imparted significantly improved moisture resistance. Oligomers containing on average two POSS units in their backbones demonstrated 72% less moisture uptake in the saturated state, compared to the control (0.58% vs. 2.1%). Moisture ingress in polyimide composites is well known to reduce T_g (in some cases as much as 100 °C), as well as thermomechanical properties, and cause blistering and delamination (composite failure) when heated. Heating experiments of moisture saturated polyimides with and without POSS revealed that, in the copolymers, very little knockdown in T_g was measured and no damaging water loss event occurred during rapid heating in direct contrast with the control material containing no POSS.

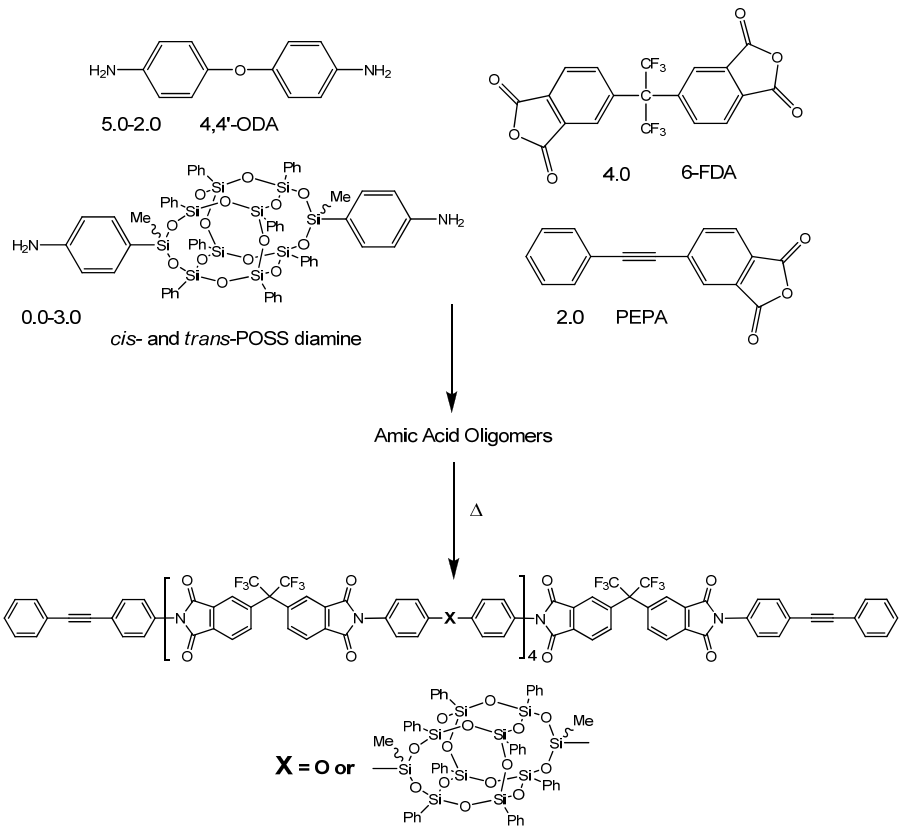

Figure 2. Reaction scheme illustrating the synthesis of 6-FDA-ODA-POSS-PEPA oligomers

Using these results as a foundation, this SEED project further investigated the subject POSS dianiline for its viability as a constituent in a polyimide chemically analogous to PMR-15 by synthesizing a nadic end-capped oligomer and characterizing its properties both in the uncured and cured states, as well as in composite form. The project strategy consisted of demonstrating that POSS, when copolymerized into the backbone of a thermosetting oligoimide, delivers a property set equivalent or superior to PMR-15, in terms of processability, mechanical properties, and thermal properties including long-term TOS, with the expectation that it is a non-toxic multi-functional alternative to MDA for thermosetting polyimides. This project could set the stage for follow-on work demonstrating biocompatibility of the POSS dianiline, further oligomer design, more extensive composite fabrication and characterization, and the fabrication and testing of composite articles relevant to DoD aircraft and/or rockets. An objective of this project was to reduce the risk and improve the TRL of the organic/inorganic hybrid polyimide approach, and to set the stage for key partnerships with industrial partners such as pre-preg manufacturers and end-users such as aircraft designers/fabricators with the ultimate goal of commercialization.

Materials and Methods

This project was broken down into five technical tasks, described as follows.

Task 1: Monomer Synthesis

Referencing Figure 3, the dianiline of interest (4) was synthesized by reacting two equivalents of dichlorosilane (2) with the POSS tetrasilanol (1) in the presence of triethylamine. This generates a mixture of cis- and trans- isomers of protected POSS dianilines (3). Generally speaking, it is not necessary to isolate these protected anilines. Following the reaction between the dichlorosilane (2) and the POSS tetrasilanol (1), the trimethylsilyl groups are cleaved from the crude product (3) to produce POSS dianilines (4), which are isolated by filtration. The mixture of cis and trans POSS isomers can be isolated through crystallization techniques. Isomer geometry has been discovered to affect oligomer processability, specifically viscosity, but not delivered properties in the cured state, thus isomer isolation was not pursued. The cis/trans POSS isomer mixture has been established to afford the best balance of processing and delivered properties. A suitable quantity of the POSS dianiline to facilitate all other tasks was synthesized in this task. Although only 10 g batches were produced prior to this project, scale up to larger quantities did not pose significant challenges. The synthesis method depicted in Figure 3 is described below.

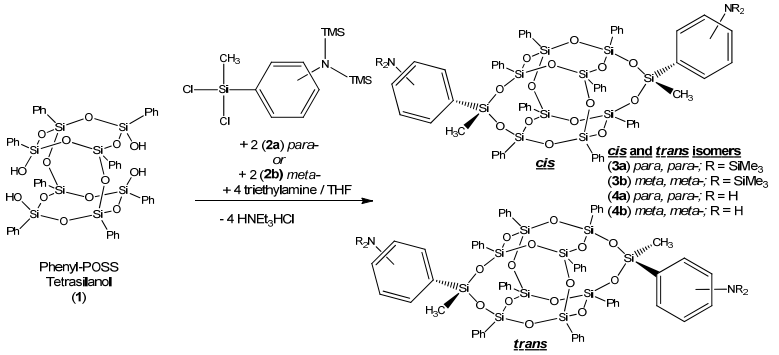

Figure 3. Reaction scheme used to synthesize POSS diamine monomer from core tetrasilanol.

Task 1: Synthesis Method Details

4-[Bis(trimethylsilyl)amino]phenyltrichlorosilane (2a): A solution of 4-Bromo-N,N-bis(trimethylsilyl)aniline (9.48 g, 30 mmol) in 25 mL of anhydrous THF was placed in an addition funnel and slowly added to a stirring mixture of Mg (0.912 g, 38 mmol) and anhydrous THF initiated with a crystal of I2 and a drop of 4-Bromo-N,N-bis(trimethylsilyl)aniline. The reaction was allowed to stir overnight at ambient temperature, cannulated to a 250 mL round bottom flask, and slowly added to a stirring mixture of THF (10 mL) and silicon tetrachloride (5.35 g, 31.5 mmol). This was allowed to stir overnight. The solvent was removed in vacuo from the reaction mixture and dry hexane was added to extract the product by filtration through celite. After removing all volatiles under a dynamic vacuum, the residual yellow colored filtrate was transferred to a 25 mL flask and distilled under dynamic vacuum to give the product, as a colorless, viscous liquid in 90% yield. 1H NMR (CDCl3, δ) 0.16 (s, 18H, NSiMe3), 7.08 (m, 2H), 7.73 (m, 2H) ppm. 13C NMR (CDCl3, δ) 2.50, 126.09 (Cγ), 130.34 (Cα), 134.03 (Cβ), 153.89 (Cδ) ppm. 29Si NMR (CDCl3, δ) -0.74 (SiCl3), 5.53 (SiMe3), (ratio = 1:2) ppm.

Phenyl-POSS trisilanol [Ph7Si7O9(OH)3] (1) was obtained from Hybrid Plastics and used as received. Under a nitrogen atmosphere, in a 50 mL round-bottom flask, phenyl POSS-tetrasilanol (1), $Phenyl_8Si_8O_{10}(OH_4)$ (2.00g, 1.87 mmol) was suspended in 10 mL of anhydrous THF. To this stirred suspension, a solution of 4-[bis(N,N-trimethylsilyl)phenylamino] methyldichlorosilane (1.376 g, 3.93 mmol) and NEt_3 (0.776 g, 7.67 mmol) in THF (10 mL) was

slowly added in a drop-wise manner. After 30 minutes, the solution was filtered to remove NEt_3HCl (974 mg, 7.08 mmol, 95 % theoretical) and the solvent was removed under vacuum. Approximately 1 mL of diethyl ether was added to the product followed by 20 mL of MeOH to produce a suspension of white-colored intermediate. The trimethylsilyl groups were hydrolyzed by the addition of 1 drop of concentrated acetic acid and 1 hour of stirring. Equal-molar amounts of *cis*- and *trans*-products were isolated by filtration and dried under a nitrogen stream to give a white powder (3a) in 77 % yield (1.922 g, 1.44 mmol). ^{1}H NMR ($CDCl_3$, δ) 0.11 (s, 6H, CH_3), 3.3 (broad s, 4H, NH_2), 6.60 (m, 4H), 7.10 to 7.83 (m, 44H) ppm. ^{13}C NMR ($CDCl_3$, δ) *cis*-product -0.31 (CH_3), 114.62 (aniline-C_γ), 124.90 (aniline-C_α), 127.33, 127.66, 127.74 (Ph-C_γ, ratio = 2:2:4), 130.06, 130.28, 130.33 (Ph-C_δ, ratio = 2:4:2), 130.75, 131.19, 132.06 (Ph-C_α, ratio = 2:2:4), 134.02, 134.11, 134.18 (Ph-C_β, ratio = 4:2:2), 134.96 (aniline-C_β), 147.52 (aniline-C_δ); *trans*-product -0.29 (CH_3), 114.76 (aniline-C_γ), 125.11 (aniline-C_α), 127.50, 127.74 (Ph-C_γ, ratio = 4:4), 130.20, 130.29, (Ph-C_δ, ratio = 4:4), 130.96, 132.05 (Ph-C_α, ratio = 4:4), 134.02, 134.14, (Ph-C_β, ratio = 4:4), 134.96 (aniline-C_β), 147.28 (aniline-C_δ) ppm. ^{29}Si NMR ($CDCl_3$, δ) *cis*-product -79.4, -79.1, -78.2, -29.7 (ratio 2:2:4:2); *trans*-product -79.3, -78.2, -29.7 (ratio = 4:4:2) ppm. Elemental analysis, found (calculated): C, 55.29 (55.74); H, 4.37 (4.38); N, 1.99 (2.10).

Task 2: Oligomer Synthesis (*Tasks 2-3 are iterative)*

In this task, PMR oligomers were synthesized by two different strategies. Nadic endcaps were utilized in all routes to preserve the resin curing temperature characteristics of PMR-15. The two basic approaches are illustrated in Figures 4 and 5, respectively. In the primary strategy, the POSS dianiline simply replaced MDA in the heritage PMR-15 chemistry. Because the POSS monomer is larger than MDA, it was expected to increase the molecular weight between crosslinks which was in turn expected to reduce T_g in similar fashion to what had been previously observed. To mitigate this reduction in T_g, we investigated varying oligomer length (n) between 0 and 2, as shown in Figure 4, to effectively increase the crosslink density of cured oligomers. The 2N oligomer is derived from equivalent stoichiometry to that used in PMR-15. Blends of the oligomers were also investigated, in an effort to tune the crosslink density and T_g.

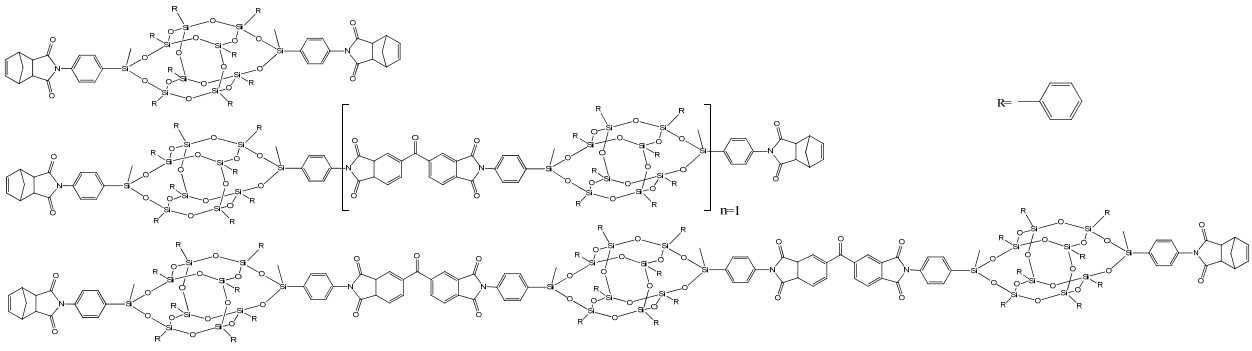

Figure 4. Reaction Scheme 1: target PMR oligomers featuring NE, BTDE, and POSS substituted for MDA with varying repeat units n (BTDA-POSS); 0N (top), 1N (middle), and 2N (bottom).

The nomenclature for the group of oligomers investigated in this program and used in the remainder of this report is shown in Table 1. A repeat n is represented by BTDA or BTDE and a dianiline.

Table 1. Oligomer nomenclature utilized for the purposes of this report.

The constituent monomers are BTDA (benzophenonetetracarboxylic dianhydride), BTDE (benzophenonetetracarboxylic diester), MDA (methylene dianiline), and POSS (polyhedral oligomeric silsesquioxane).

$BTDE_2MDA_3NA_2$	PMR-15 (MeOH)
$BTDA_2MDA_3NA_2$	PMR-15 (THF)
$POSS_1NA_2$	0N
$BTDA_1POSS_2NA_2$	1N
$BTDA_2POSS_3NA_2$	2N

PMR-15 Synthesis in Methanol~5g Scale: In a dry nitrogen purged glove box, 2.016g 3,3',4,4'-benzophenonetetracarboxylic dianhydride (BTDA) and 0.985g 5-norbornene-2,3-dicarboxylic anhydride were weighed in a 50mL round bottom flask. The flask was removed from the glove box and 17mL methanol (MeOH) was added. The mixture was refluxed at 70 °C for 2 hours, during which the powders were solubilized into a yellow liquid. The solution was removed from the heat and allowed to cool to room temperature. Once at room temperature, 1.836g 4,4' methylene diamine (MDA) was added while stirring. The MDA dissolved in approximately five minutes and the solution (darker shade of yellow) was left to stir for 1 hour. The solvent was then evaporated using a Rotovap and 5.218g yellow amic acid powder was recovered. To imidize, the powder was then added to a petri dish and placed into a 200 °C oven for 2 hours, then 230°C for 30 minutes to yield an orange powder.

PMR-15 Synthesis in THF~5g Scale: In a dry nitrogen purged glove box, 1.8363g methyl dianiline (MDA) was dissolved in 10mL tetrahydrofuran (THF), 2.0159g 3,3',4,4'-2,3-benzophenonetetracarboxylic dianhydride (BTDA) was dissolved in 70mL THF, and 0.9851g 5-norbornene-2,3-dicarboxylic anhydride (NA) was dissolved into 10mL THF, in separate round-bottom flasks. The BTDA solution was poured slowly (but not dropwise) into the MDA solution while stirring. When added, the solution became orange in color and when all of the solution was added a pale yellow precipitate appeared. Then, the NA solution was added in the same manner with no apparent change in color or solubility. This was left to stir overnight. The next day, the solution was a clear yellow liquid. The solvent was evaporated using a Rotovap and 4.1090g yellow amic acid powder was recovered. To imidize, the powder was then added to a petri dish and placed into a 200°C oven for 2 hours, then 230°C for 30 minutes to yield an orange powder.

2N Synthesis in THF~3g scale: In a dry nitrogen purged glove box, three solutions were made: 2.468g meta/para POSS dianiline with 25mL tetrahydrofuran (THF), 0.202g 5-norbornene-2,3-dicarboxylic anhydride (NA) with 2mL THF, and 0.397g 3,3',4,4'-benzophenonetetracarboxylic dianhydride (BTDA) with 4mL THF. While stirring, the BTDA solution was added to the POSS dianiline solution. The solution became yellow and darkened as more solution was added. After 1 hour of stirring, the NA solution was added and no change in appearance occurred. This was left to stir overnight. The yellow solution was then evaporated using a Rotovap and 2.423g yellow amic acid powder was recovered. To imidize, the powder was then added to a petri dish and placed into a 200°C oven for 2 hours, then 230°C for 30 minutes to yield an orange powder.

1N Synthesis in THF~3g Scale: In a dry nitrogen purged glove box, three solutions were made: 2.468g meta/para POSS dianiline with 25mL tetrahydrofuran (THF), 0.303g 5-norbornene-2,3-dicarboxylic anhydride (NA) with 2mL THF, and 0.298g 3,3',4,4'-benzophenonetetracarboxylic dianhydride (BTDA) with 4mL THF. While stirring, the BTDA solution was added to the POSS dianiline solution. The solution became yellow and darkened as more solution was added. After 1 hour of stirring, the NA solution was added and no change in appearance occurred. This was left to stir overnight. The yellow solution was then evaporated using a Rotovap and 2.423g yellow amic acid powder was recovered. To imidize, the powder was then added to a petri dish and placed into a 200°C oven for 2 hours, then 230°C for 30 minutes to yield an orange powder.

POSS di-Nadic Synthesis (0N) in THF~3g Scale: In a dry N2-environment glove box, 2 solutions were made: 2.461g POSS dianiline with 25mL tetrahydrofuran (THF) and, 0.605 5-norbornene-23-dicarboxylic anhydride (NA) with 6mL THF. While stirring, the NA solution was added to the POSS solution with no change in color (clear). The solution was left to stir overnight. The solution was then evaporated using a Rotovap and 2.490 g white amic acid powder was recovered. To imidize, the powder was then added to a petri dish and placed into a 200°C oven for 2 hours, then 230°C for 30 minutes to yield an orange powder.

In the second approach, a set of monomers that deviates from those used to synthesize PMR-15 were used. As shown in Figure 5, we oligomerized phthalic anhydride (PA), a mixture of diamines including p-phenylenediamine (used in NASA's PMR-II) and the POSS diamine, reactively end-capping with nadic anhydride (NA). The combination of PA and PDA is typically precluded from use in PMR chemistries due to the comparative intractability (high viscosities) of their product oligomers, although the resultant polymer exhibits very good thermal stability and high T_g. The POSS dianiline was expected to offset the rigidity of the PA-PDA imide group because, although the inorganic core is constrained by its polycyclic character, it is relatively flexible for a polyhedral silsesquioxane, yet quite thermally stable due to the strength of the Si-O bond and its aromatic peripheral character, and moreover, the molecule itself is a very effective processing aid as it prevents inter-chain packing. Although in the scheme presented in Figure 5 the repeat unit n is on average 1.0, the ratios of POSS, PA, and PDA can be tailored to deliver specific properties and mimic the crosslink density of PMR-15. Finally, although PDA is a low molecular weight diamine, studies have not shown it to be carcinogenic by oral or dermal exposure, and the EPA has not classified PDA as such. The general synthetic procedure consisted of adding PA to a mixture of the two amines in a common solvent followed by addition of the end capping agent. As is the case for PMR-15, the product of this reaction was an oligoamic acid. The amic acid was thermally imidized either in solution or after product isolation to yield oligoimides.

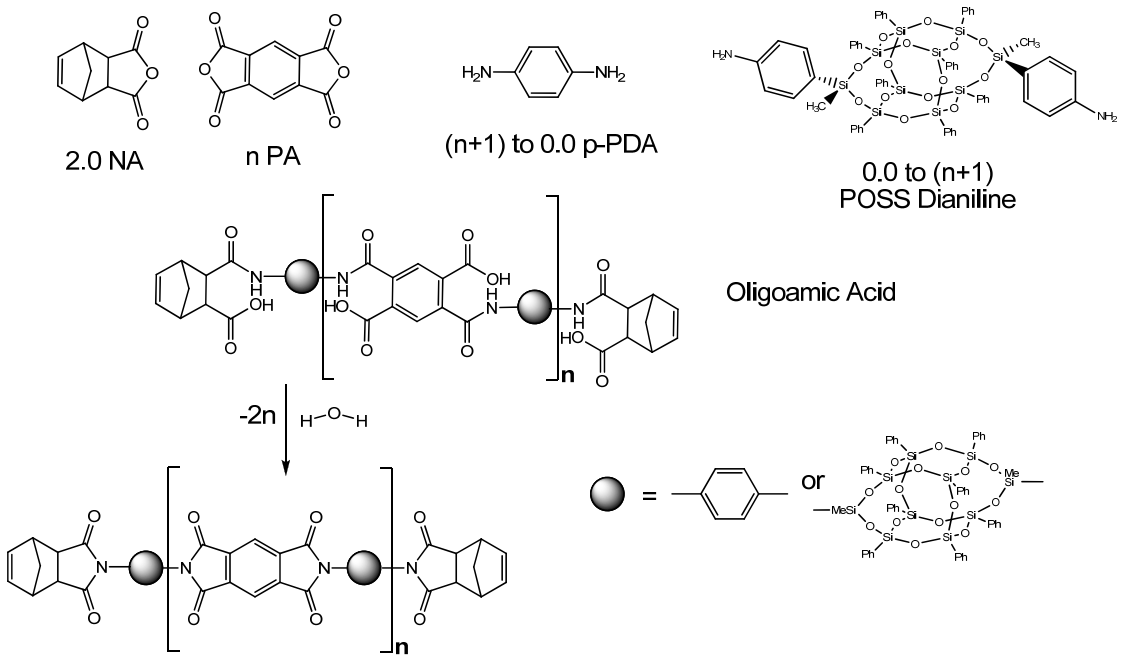

Figure 5. Reaction Scheme 2 illustrating the synthesis of oligomers from monomers that deviate from those used in PMR-15.

The use of the POSS monomer is expected to afford the ability to use rigid monomers such as phthalic anhydride (PA) and p-phenylene diamine (p-PDA) whose combination typically yields intractable polyimides but are thermally stable and feature a high Tg. In addition, the chosen monomers are non-carcinogenic and have strong supply sources within the U.S as they are used in various commercial products.

Task 3: Resin Characterization

Although an extensive database exists on the properties of PMR-15, the properties of PMR-15, synthesized in our laboratory, were analyzed in parallel, as the control material, to validate our methods. In general, polymers demonstrating a knockdown of 5% in any of the key aforementioned properties were to be eliminated as potential candidates. Alternatively, chemistries that delivered properties within 5% or were shown to be superior to those of PMR-15 were to be chosen for composite fabrication and characterization in the next task of the project. Oligoimides resulting from Task 2 were characterized for their chemical makeup by NMR. Viscosity characteristics, a measure of processability, were analyzed by parallel plate rheometry. The thermally driven curing reaction of the nadic end groups were monitored by DSC and melt rheometry techniques. Neat resin specimens were compression molded at 315 °C for 2 hours at 200 psi following lower temperature isothermal steps to promote volatile removal and imidization. Cured specimens were analyzed for their short-term decomposition and degradation products in inert and oxidizing atmospheres using TGA-MS, while long-term oxidative aging studies were performed at 316 °C for up to 700 hours in an aging oven with 1 atm circulating air, monitoring weight loss. The viscoelastic properties of cured disks including T_g were evaluated by TMA. Moisture diffusion and saturated uptake were quantified by boiling water immersion. Selected key properties of PMR-15, collected from literature sources, are shown in Table 2. These properties were used as rapid screening criteria in an iterative process between Tasks 2 and 3. The thresholds for those properties are shown in the last column, and are in general 95% of the literature values with the exception of the T_gs and TGA thermal stability. The oligomer system that best

met these criteria was selected for synthesis scale up to 300 g from which a composite panel was fabricated in Task 4.

Table 2. Key properties of PMR-15 resin gathered from literature, their measurement techniques, and threshold properties that will be used to screen new resin formulations.

indicates critical property that was used for screening.

Property	**Literature**	**Measurement Technique**	**Screen Threshold**
Zero Shear Viscosity (@ 150 °C, P)	1.16×10^6	Parallel Plate Rheometer	$\leq1.3\times10^6$
T_g (°C, no postcure)	299	TMA	≥299
T_g (°C, postcured in air at 316 °C for 24 hrs)	333	TMA	≥333
Weight Loss (% @ 316 °C/400 hrs in air)	1.88	Oven Aging/Gravimetric	≤1.97
Weight Loss (% @ 316 °C/500 hrs in air)	4.97	Oven Aging/Gravimetric	4.72
5% Weight Loss Temperature (°C, 1 °C/min ramp, N_2 purge	440	TGA	≥440
Coefficient of Thermal Expansion (μm/mm·°C)	55	TMA	-
Moisture Uptake (100 hrs, 80 °C/80 RH)	4.0	Humidity Chamber/Gravimetric	≤4.0

Characterization Methods

Nuclear Magnetic Resonance (NMR) Spectroscopy

All 1H and 13C NMR spectra were obtained from a Bruker 300 FT-NMR 300MHz. DMSO-d6 was used as the solvent.

Differential Scanning Calorimetry (DSC)

DSC experiments were carried out on a TA Instruments Q200. T-Zero DSC pans were loaded with 10-20mg of imide powder. The experiments were performed under a nitrogen environment at a purge rate of 50mL/min. An initial ramp of 10 °C/min to 250 °C from RT was implemented to eliminate any residual solvent or water and to allow the powder to flow to form good contact with the bottom of the pan. The samples were then equilibrated at 40 °C and ramped again at 10 °/min to 315 °C. The material was then held at this temperature for 2 hours to promote curing and subsequently equilibrated at 40 °C. The final temperature ramp was done at 10 °/min to 400°C.

Thermal Gravimetric Analysis (TGA)

TGA experiments were performed on a TA Instruments Q5000. Experiments were conducted under both air and nitrogen atmospheres. Temperature ramps were implemented between 25°C and 600°C at a rate of 1 °C/min.

Rheology

Rheological experiments were carried out on a TA Instruments Discover DHR3. The samples were loaded onto 25mm stainless steel parallel plates with a gap of 0.750mm. During the oscillatory experiments, the strain amplitude was set to 1% and angular frequency was ramped from 0.1 to 100 rad/s. All experiments were carried out at 250°C.

Thermomechanical Analysis (TMA)

TMA experiments were conducted using a TA Instruments Q400. A quartz expansion-type probe was used and the furnace was purged with a nitrogen atmosphere. Initially, a force of 0.2000N was implemented and the temperature was equilibrated at 100°C. Force was modulated at 0.05Hz at an amplitude of 0.10N. The temperature was then cycled between 200°C and 100°C for two iterations. The temperature was then ramped at 5 °C/min to 360-400°C, cooled at 5 °C/min to 100 °C, and again ramped at 5 °C/min to 360-400°C. The cured glass transition temperature was ascertained from the last temperature ramp.

Density

Density measurements were performed using a Mettler-Toledo Density Kit on an MS-S Analytical Balance. The liquid used was ethanol. Three measurements were taken and the average is presented.

Moisture Uptake

A 2L Erlenmeyer flask was filled with approximately 1750mL of de-ionized water and heated until boiling. Specimen discs were thoroughly dried in a vacuum oven for 3 days or until weight stabilization occurred. All specimens were weighed and then placed into the flask. At approximately 1 hour intervals, the samples were removed from the boiling water, blotted dry with paper media, blown dry with nitrogen, and weighed. The samples were then placed back into the boiling water and the process was repeated until the eighth interval at which time the samples were left overnight in boiling water before the final weight measurement.

Long-Term Thermo-Oxidative Stability (TOS)

Long-term isothermal TOS experiments were conducted in a Lindberg Blue M tube furnace, at 316°C. An air-generator fitted with a flow meter was connected to the tube such that a continuous flow of 100ml/min of air flowed across the samples. The cured discs were placed onto a graphite boat which was wrapped in either an aluminum or copper mesh to provide support to the discs and to facilitate gas flow above and below the samples. Disk mass measurements were

taken at 3-4 day intervals. Figure 6 shows the tube furnace and samples atop aluminum mesh on the graphite boat.

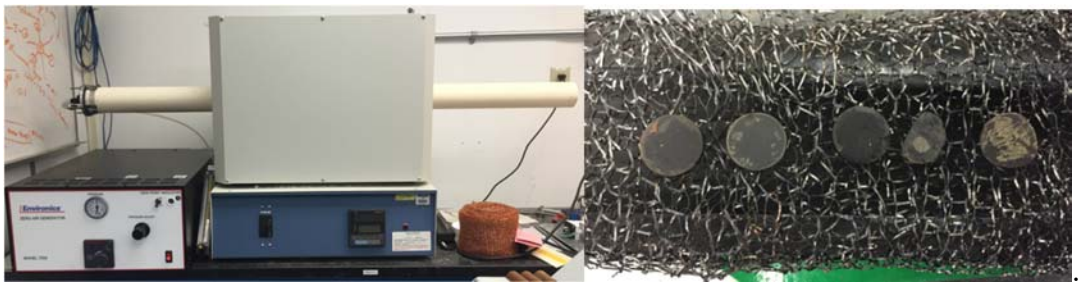

Figure 6. (Left) Lindberg Blue M tube furnace and air generator used for long-term TOS experiments, and (Right) cured neat resin discs on aluminum mesh wrapped around a graphite boat.

Task 4: Composite Fabrication

In this task, two 4in×4in×0.1in flat laminate composite panels comprised of PMR-15 and the selected resin from (3) in combination with Hexcel IM7, 4 harness satin weave, GP sized carbon fiber woven fabric, were fabricated by curing pre-preg consisting of the fabric plies coated with the resin of interest. Each panel required approximately 35 g of resin. The panels were sectioned for characterization in Task 5 using a rotary diamond wheel with water as the cooling medium. Fifty weight percent solute solutions in methanol for PMR-15, and in THF for the POSS oligomide, were made. Fabric plies cut to the prescribed dimensions were dip coated in these solutions and dried to render pre-preg. In accordance with ASTM D 5687 *Standard Guide for Preparation of Flat Composite Panels with Processing Guidelines for Specimen Fabrication*, resultant plies were stacked in a steel mold to the desired part thickness and cured under pressure by compression molding using the predetermined processing cycle from the preceding characterization efforts, and the commercially recommended cycle for PMR-15. After cure, the parts were removed and systematically characterized in Task 5.

Task 5: Composite Characterization

Elementary composite data on the resultant panels from Task 4 were collected in this stage of the project. Void content, T_g, and flexural (ASTM D 7264) and interlaminar shear (ASTM D 2344) mechanical properties were evaluated after sectioning the panel into test specimens using a diamond wheel composite rotary saw. Mechanical property testing was performed on a 300 kN Tinius Olson load frame. A long-term TOS aging study was also performed, up to 700 hours at 316 °C. Key composite properties for PMR-15/T650-35, obtained from published articles, are shown in Table 3. In general, achievement of 95% of the value for the thermal properties and 90% of the mean value of the mechanical properties indicate positive results. T650-35 fabric was not available for this effort. Therefore, Hexcel IM7 4 harness satin weave carbon fiber fabric with GP (high temperature epoxy sizing) was utilized.

Table 3. Key properties of PMR-15/T650-35 composites gathered from literature, their measurement techniques, and threshold properties that will be used to screen new resin formulations for their delivered composite properties.

Property	**Literature**	**Measurement Technique**	**Threshold**
T_g (°C, G′ onset)	348	DMA	340
T_g (°C)	346	TMA	340
Flexural Strength (MPa, 23 °C)	1082 ± 89	ASTM D 7264	1028
Flexural Modulus (MPa, 23 °C)	58 ± 2	ASTM D 7264	55
Flexural Strength (MPa, 288 °C)	747 ± 66	ASTM D 7264	710
Flexural Modulus (MPa, 288 °C)	57 ± 2	ASTM D 7264	54
Interlaminar Shear Strength (MPa, 23 °C)	61 ± 2	ASTM D 2344	58
Interlaminar Shear Strength (MPa, 288 °C)	43 ± 2	ASTM D 2344	41
Weight Loss (% @ 288 °C, air, 1000 hrs)	0.77	Oven Aging/Gravimetric	0.81
Weight Loss (% @ 288 °C, air, 1500 hrs)	1.05	Oven Aging/Gravimetric	1.10

Results and Discussion

Task 2: Oligomer Synthesis

After the synthesis of PMR-15, 0N, 1N, and 2N, they were characterized by 1H, 13C, and 29Si solution-based NMR to ascertain the molecular compositions of the reaction products. The chemical structures of each of the target oligomers are represented in Figure 7. To compare the target theoretical molecules with the synthesis products, peaks corresponding to classes of protons in the 1H NMR spectra for the oligoamic acids prior to imidization were integrated and normalized to the protons in the norbornyl rings in the end caps, and compared with theoretical values. This normalization strategy was chosen because all oligomers should be terminated with norbornyl groups, thus there should be 4 total protons of either aforementioned type for each molecule, and normalization should render an average number molecular weight (M_n). For PMR-15, the integrations were normalized to the two protons in the methylene of bridge of the norbornyl group (coded purple in Figure 7), while for the POSS-containing materials, normalization was performed through the protons on the ethane groups (red). An example of a 1H NMR spectra for the 0N oligoamic acid is shown in Figure 8. The results of normalized integration are presented in Table 4 for PMR-15 and Table 5 for the POSS-containing oligomers. In general, very good agreement was found with the exception of the protons associated with the amic acid group (color coded dark blue and orange for the amine and hydroxyl/carboxylic acid groups, respectively), and in some cases the protons attached to phenyl rings. The former finding is likely due to coupling interactions with the carrier solvent, and/or the existence of methoxy groups formed during BTDA esterification, that skew the integrations. Regarding the protons associated with phenyl rings, which are measured to be significantly higher than theoretical (~by 1.5), are located within the spectral range of 6.6-8.3 ppm which is tightly packed due to the number of protons with similar electronic environments, possibly leading to errors with software integration, or the average molecular weight between terminal groups is skewed high due to abnormal polydispersity, or the average molecular weight is indeed higher than that targeted. The protons coded as green are also measured to be higher than theoretical, and since those protons are either associated with the norbornyl groups and the methylene bridge of MDA, any variance should be associated with increased molecular weight due to the presence of higher than expected MDA segments. Despite the possibility of high molecular weight, the cured glass transition of the PMR-15 synthesized in this study is the same as that reported in the literature, which will be discussed later in the resin characterization section, and unlike PMR-15, this series of oligomers was synthesized in THF due to the insolubility of the POSS monomer in methanol.

The POSS-containing oligoimides provide additional insight into the nature of this chemistry. The expected and measured integrations for 0N are in very good agreement, while those of 1N and 2N suggest higher average molecular weight than that which was targeted. It is possible that the use of BTDA, not present in 0N, is complicating to the chemistry. Nonetheless, this NMR analysis provides reasonable confidence that the target molecules were successfully synthesized without significant compositional anomalies, and target average molecular weights were achieved or exceeded.

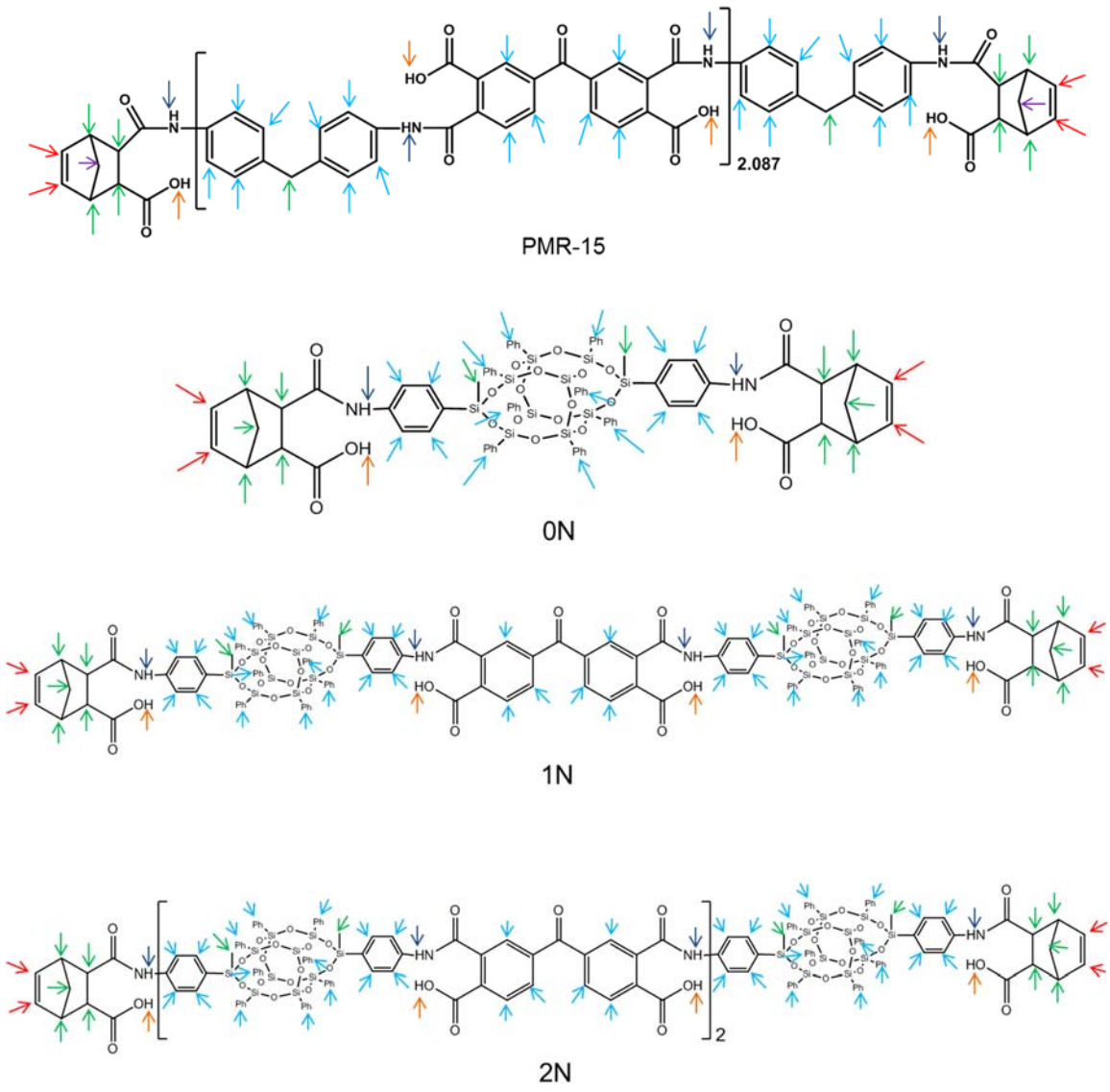

Figure 7. Molecular structures of the amic acids of PMR-15, 0N, 1N, and 2N. Colored arrows correspond to the NMR assignments in Tables 3 and 4.

It is also very informative to examine the 29Si spectra for the POSS-containing materials in relation to the spectra for the POSS dianiline starting material, as it provides diagnostic information pertaining to the integrity of the POSS cage throughout the various stages of material treatment, including the synthesis of the oligoamic acids and the thermal imidization of the amic acid groups. This diagnostic is also aided by the simplicity of the spectra, as shown in Figure 9, where three regions of peaks are prevalent. The T silicon atoms (those with attached phenyl groups and three oxygen bonds) exhibit peaks in the -78 to -80 ppm region, while the D silicon atoms (two oxygen bonds) are identified by the peak at -30 ppm. In terms of chemical and presumably thermal stability, the T atoms are more stable than the D atoms, and Si-C bonds are weaker than Si-O. Cage integrity can be compromised by the presence of basic groups, especially at elevated temperature, therefore thermal imidization was identified as a high risk at the inception of the program. During imidization, oligoamic acid is heat treated at 200 °C for 2 hours and 230 °C for

30 minutes, where the amic acid ring closes to form an imide group, liberating water and methanol, both being basic species that can attack the D silicon atoms. However, as can be seen in Figure 9, the NMR spectra reveal that the D silicon atoms' electronic environment remains largely unchanged during oligomer synthesis and thermal imidization, representing a very positive result.

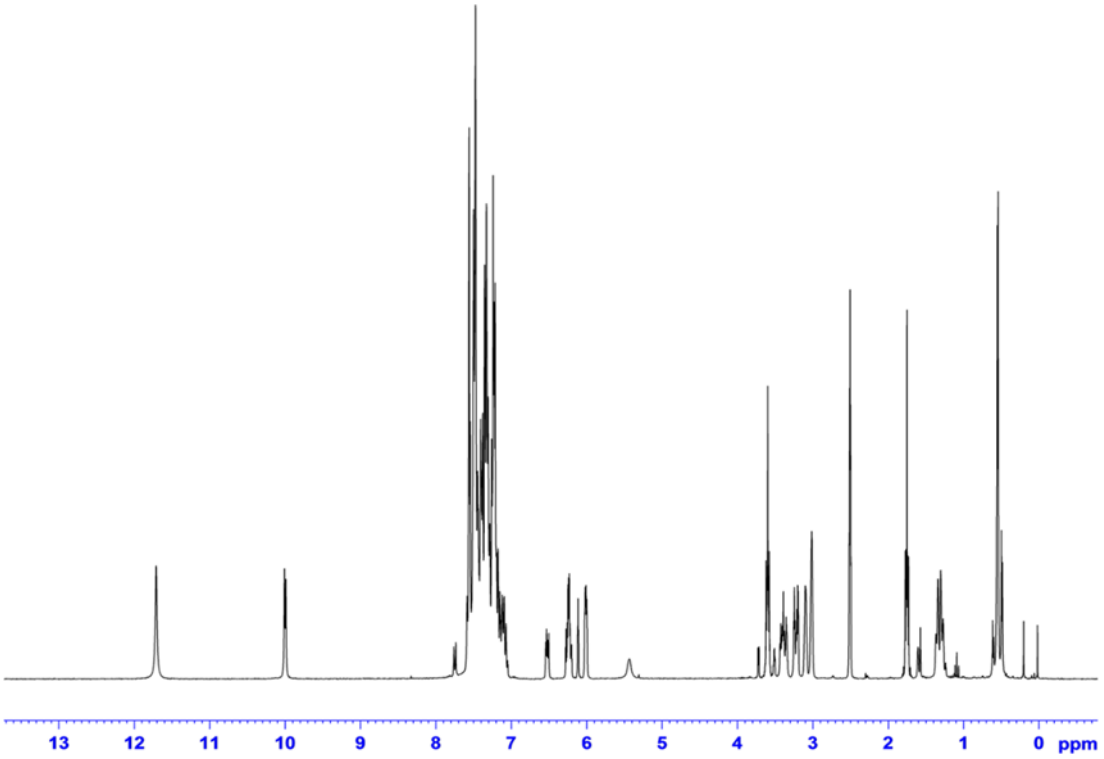

Figure 8. 1H NMR spectra for 0N oligoamic acid. The region between 7-8 ppm features the highest intensity and greatest concentration of peaks due to the number of protons covalently attached to phenyl groups.

Table 4. Expected and measured integrated 1H NMR peak intensities for the PMR-15 oligoamic acid.

	PMR-15 (MeOH)		PMR-15 (THF)	
Region	Expected	Measured	Expected	Measured
6.0 – 6.25ppm	4	4.96	4	4.06
6.6 – 8.3ppm	37.22	58.33	37.22	41.68
1.25ppm	4	4	4	4
2.9 - 3.45ppm; 3.7 - 4.0ppm	14.17	15.92	14.17	14.53
9.8ppm	6.17	1.43	6.17	1.93
10.5ppm	6.17	0.12	6.17	4.40

Table 5. Expected and measured integrated 1H NMR peak intensities for the 0N, 1N, and 2N oligoamic acids.

	0N		1N		2N	
Region	Expected	Measured	Expected	Measured	Expected	Measured
5.9 – 6.3ppm	4	4	4	4	4	4
7.0 – 8.0ppm	48	48.45	102	108.63	156	169.14
0 – 1.6ppm; 3.0-3.5ppm	18	17.92	24	28.80	30	35.65
10ppm	2	1.51	2	0.64	6	0.71
11.75ppm	2	1.97	2	1.82	6	3.76

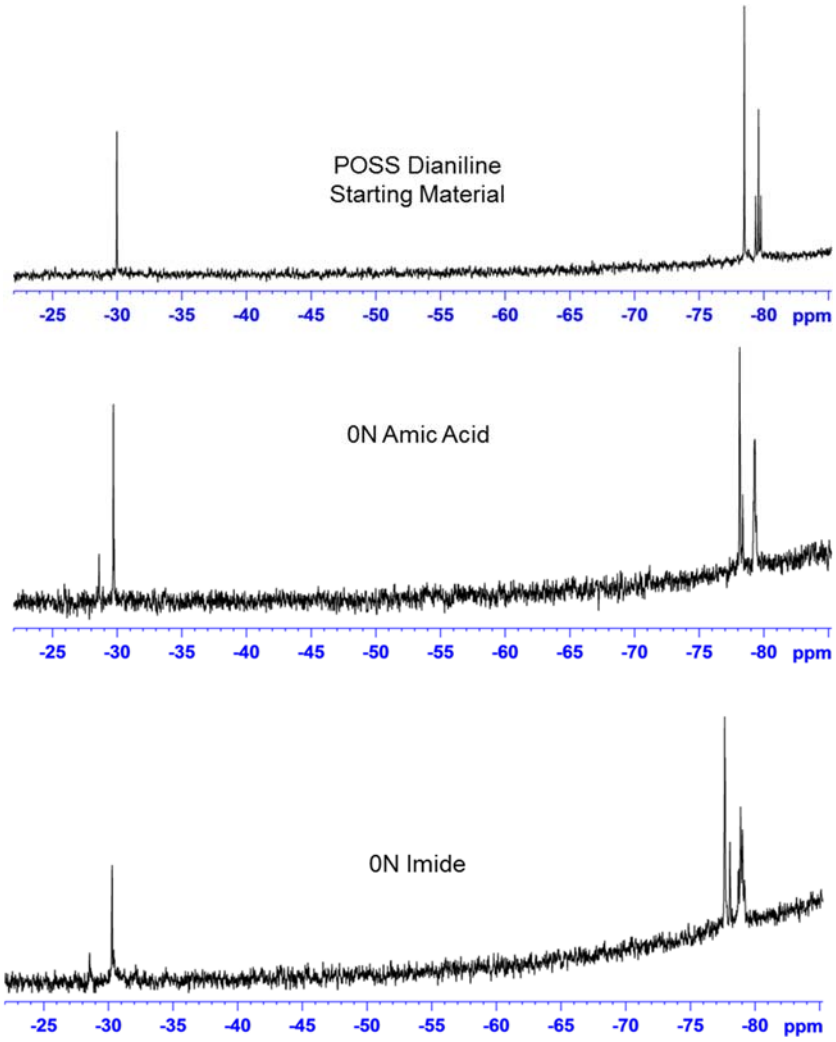

Figure 9. 29Si NMR spectra for the POSS dianiline starting monomer, 0N amic acid, and 0N imide.

Task 3: Resin Characterization

Powder Characterization

Differential scanning calorimetry (DSC) was used to provide an initial assessment of pre-cure and post-cure (after 315 °C for two hours in gaseous nitrogen) glass transition temperatures (T_gs), identified by an inflection in the heat flow signal. The thermograms corresponding to the uncured oligoimides after an initial ramp to 250 °C to eliminate any residual solvent are shown in Figure 10. In all four materials, inflections are clearly visible indicating a transition from glassy to more fluid-like behavior. The T_g of PMR-15 is 200 °C, equivalent to that reported in the literature [1]. Co-oligomerization with POSS dianiline, replacing MDA, reduces the T_g as a function of POSS content (2N>1N>0N), but this observation also must have dependencies on oligomer molecular weight (2N>1N>0N) and inter-molecular packing. Although the heat capacities of the oligoimides were not quantified in this effort (requiring modulated DSC or resolving data from thermograms run at several heating rates), it is evident from the amount of heat flow required during the scan of each material that significant differences exist. In terms of

average molecular chain length, 2N is most similar to PMR-15 but requires much more energy than PMR-15 to heat at 10 °C/minute. This is likely a combination of the significantly higher molecular weight of the POSS segments (requiring more energy to excite) in relation to MDA, and also may be influenced by inter-molecular packing which is expected to be of lower efficiency in the POSS-containing oligomers due to high volume occupation of the POSS segments. The 0N oligomer exhibits a qualitatively lower heat capacity than 1N and 2N, most likely due to its relatively short chain segments. These results suggest that processability reflected by flow viscosity as a function of temperature is reduced and thereby positively influenced by POSS.

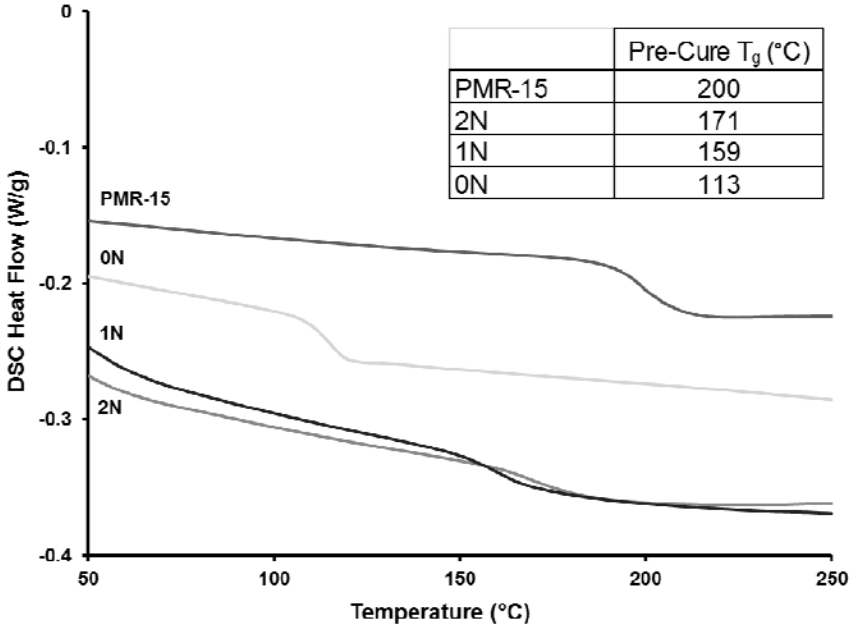

Figure 10. Differential scanning calorimetry (DSC) thermograms of all uncured oligoimides. Quantified pre-cured glass transitions are tabulated in the inset.

The post-cure DSC thermograms of the same specimens after heat treatment at 315 °C for two hours (recommended cycle for PMR-15) are plotted in Figure 11. Again, the T_g of PMR-15 is equivalent to that reported in the literature (339 compared to 333 °C). Immediately following the transition, the PMR-15 signal becomes exothermic, likely caused by residual cure occurring after strong segmental motion is induced, but is more strongly a result of the inception of network degradation first through the products of norbornyl cross-linking [24]. In comparison, the T_gs of the POSS-containing cured thermosets are weak and difficult to discern, especially for 1N and 0N, presumably due to their relatively higher crosslink densities resulting from having shorter oligomers on average. 2N appears to exhibit a transition signal at 252 °C, significantly lower than that of PMR-15. 1N may have a T_g at 230 °C and 0N's cannot be identified. Modulated thermomechanical analysis (M-TMA) data will be analyzed later in this section, providing an alternative and more sensitive technique for transition determination. The relative weakness of the T_g signals of the POSS-containing cured networks can be linked to the sluggish thermal-induced activity of the high mass POSS cages and likely higher degrees of networking for 1N and 0N.

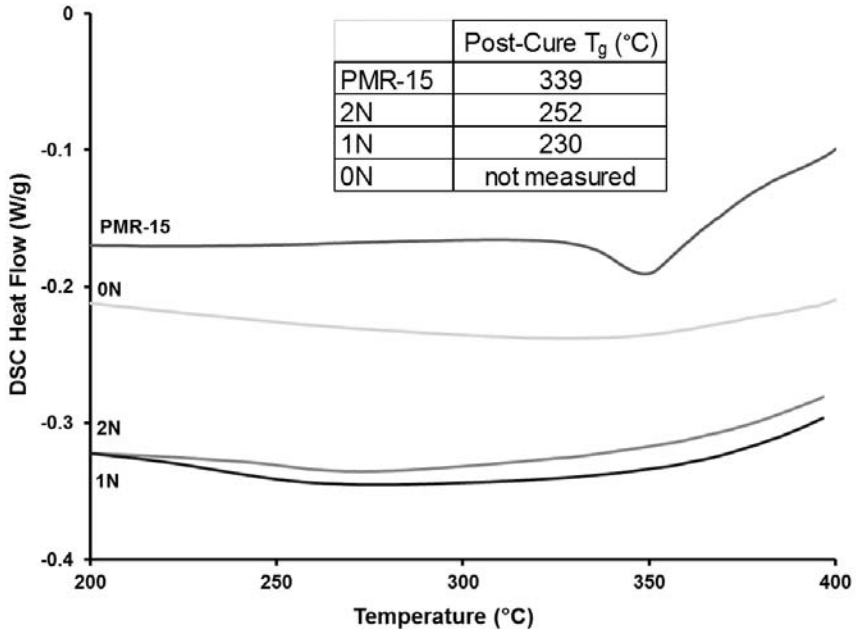

Figure 11. Differential scanning calorimetry (DSC) thermograms of all oligoimides after curing at 315 °C for two hours. Quantified cured glass transitions are tabulated in the inset.

Because of the low T_g measured for 2N in relation to PMR-15 and the suspected low value for 1N, a blending study was undertaken between 2N and 0N, and 1N and 0N, attempting to utilize cross-link density as a tool to raise the T_g of a given network. It was also postulated at this time that 0N may have a suitably high cured T_g, but due to its high cross-link density, could be unreasonably brittle for a composite resin system, so a blended system could provide a balance of beneficial end-use temperature and mechanical properties. Thus 25, 50, and 75 weight percent of 0N was blended with 1N and 2N, respectively, through the assistance of solvent (THF). The resultant powders were isolated and dried and analyzed analogously to the other materials by DSC. The pre- and post-cure T_gs are tabulated in Table 6 and plotted in Figure 12. For all of the blends, a singular pre-cure T_g is witnessed, signifying near or complete compatibility of the constituents, independent of mix ratio. For both the 1N and 2N blended systems, the pre-cure T_gs are lowered with a strong linear response to increasing 0N concentration.

Table 6. Uncured and cured glass transition temperatures, as measured by DSC, for blend of 1N and 2N, respectively, with different weight percentages of 0N.

Weight Percent 0N	0	25	50	75	100
1N Uncured	159.3	143.9	135.8	118.8	115.6
1N Cured	229.8	249			
2N Uncured	170.7	145.7	133.7	119.1	115.6
2N Cured	252.5	260.5			

In terms of measured cured T_gs for the blends, only the cured network transitions for the 25 weight present containing systems were discernable (data not shown). In these cases, the cured T_gs were increased 8 and 20 °C for 1N and 2N, respectively. It was discovered in our previous studies of 6-FDA-ODA-POSS-PE systems [22] that with higher degrees of POSS in oligomer chains, the more thermal energy was required to render what could be considered near to full cure. For this work, however, due to the relatively low thermal stability of the PMR-15 framework (BTDA as opposed to 6-FDA, and NA as opposed to PE), increased temperatures for cure was not utilized as a tool to promote further cross-linking. It is therefore plausible to expect that the POSS-containing networks are not what would be considered near or fully cured. Moreover, FTIR could not be used as a diagnostic spectroscopic tool to monitor the cure conversion of norbornyl end-caps, as there are no distinct bands corresponding to the reaction products that can be spectroscopically isolated, in contrast with phenylethynyl where the carbon-carbon triple bond has a distinct absorption band, thus facilitating analysis of the kinetics of its consumption.

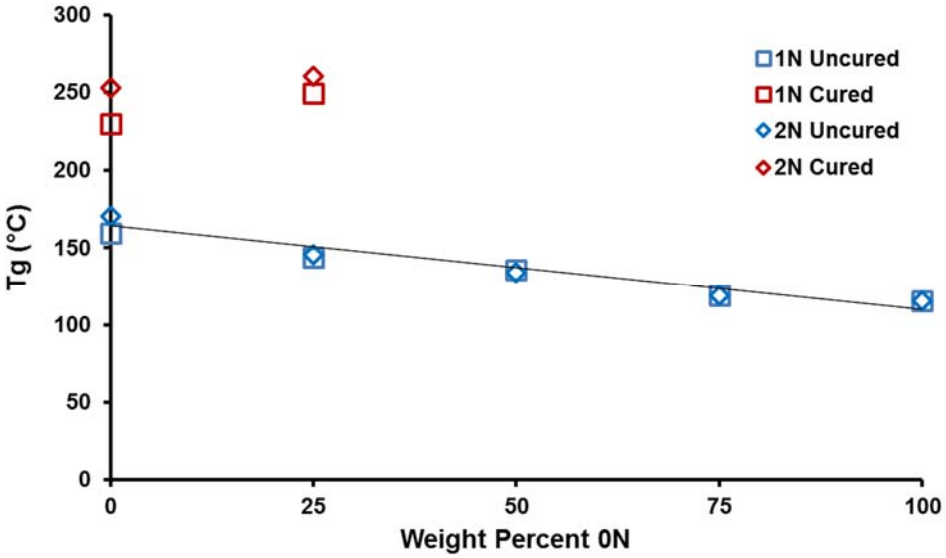

Figure 12. The dependence of uncured and cured T_g as a function of 0N mix ratio in blends with 1N and 2N, respectively. The cured T_gs of the systems containing more than 25 percent by weight of 0N could not be identified.

To gauge the thermal stabilities of this new suite of materials, cured powder (315 °C for two hours) was first analyzed by dynamic thermogravimetric analysis (TGA), at a heating rate of 1 °C/minute in inert (gaseous nitrogen) and oxidizing (air) atmospheres, to 600 °C. This slow heating rate was chosen such that an accurate depiction of decomposition events as a function of temperature could be measured. The data in nitrogen is plotted in Figures 13 and 14, for normalized residual mass and the derivative of mass loss as a function of temperature, respectively. Measurable mass loss begins to occur at ~330 °C, attributed to the disassociation of the products of the nadic crosslinking group, known to be the weakest species due to its aliphatic character [24-26]. Above 400 °C, in terms of thermal stability characterized by mass retention, the POSS-containing cured polyimides are more resistant to mass loss than PMR-15. This result suggests that POSS is a more thermally stable segment than MDA in PMR-15. At approximately 475 °C and above, the aromatic rings attached to the POSS cages can participate in co-reactions that produce robust carbonaceous byproducts, likely slowing the mass loss kinetics in that temperature

range, also resulting in significantly higher char yields at 600 °C. There is also an obvious trend amongst the POSS-containing networks: thermal stability is inversely proportional to nadic end group concentration (2N>1N>0N). In Figure 14, distinct mass loss events can be distinguished, especially for the POSS-containgin networks. For PMR-15, methylene bridge dissociation and associated combination reactions occur in concert with late nadic crosslinking degradation thereby smoothing out the profile.

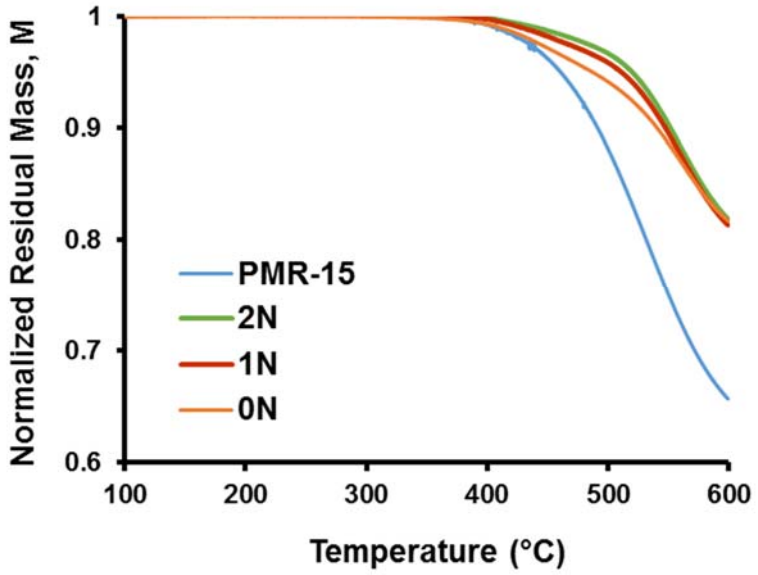

Figure 13. Normalized mass loss profiles as a function of temperature, measured by TGA at 1 °C/minute in a gaseous nitrogen atmosphere.

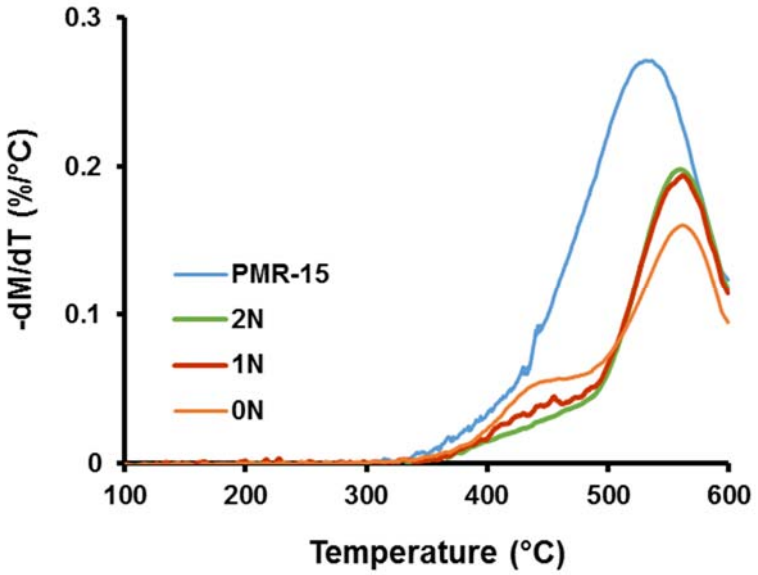

Figure 14. The derivative of mass loss as a function of temperature, measured by TGA at 1 °C/minute in a gaseous nitrogen atmosphere. The peaks designate mass loss events.

The general thermal stability trends observed during decomposition in an inert atmosphere are again observed in air in Figures 15 and 16. Under thermo-oxidative conditions above 500 °C, the POSS cage can be oxidized to render SiO_2, leaving appreciative residue at 600 °C whereas PMR-15 has been completely decomposed and volatilized. The 0N residue is of highest mass at 600 °C due to its relatively high POSS content in its cured network. Under oxidizing conditions, it has been shown by others that the decomposition of PMR-15 occurs first through the nadic crosslinked groups, followed by the methylene bridge of MDA, and lastly through BTDA [26].

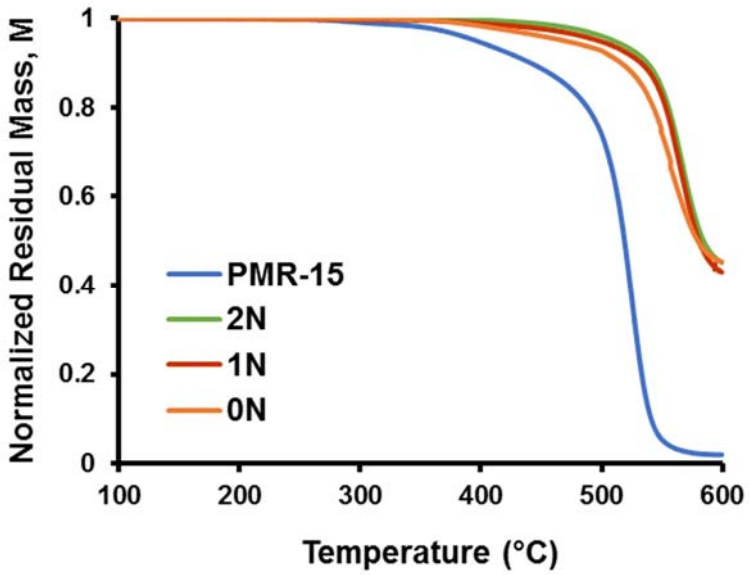

Figure 15. Normalized mass loss profiles as a function of temperature, measured by TGA at 1 °C/minute in air.

To further illustrate the dissimilarities in thermally-induced decomposition attributes and pathways between PMR-15 and the POSS-containing oligomers, the temperatures at which 5 and 10 percent mass losses ($T_{d,5}$ and $T_{d,10}$) occur in the preceding sets of TGA data in both nitrogen and air are plotted in Figure 17 as a function of nadic dianhydride monomer mass fraction. For the POSS-containing materials, these mass loss statistics are a precise linear function of nadic end group concentration, as demonstrated by R^2 values exceeding 0.99. Thus the relative thermal stabilities are 2N>1N>0N. This analysis provides further evidence that the dominant mass loss mechanism in the regime of total mass loss below 10 percent is nadic group decomposition. PMR-15 does not fit this trend. The 5 and 10 percent mass loss temperatures are much lower than expected in the context of nadic end group concentration, suggesting that an additional mass loss mechanism is active. As discovered in the work by Meador et al [26], MDA decomposition occurs early in the degradation process, and the POSS dianiline must therefore be a more stable species.

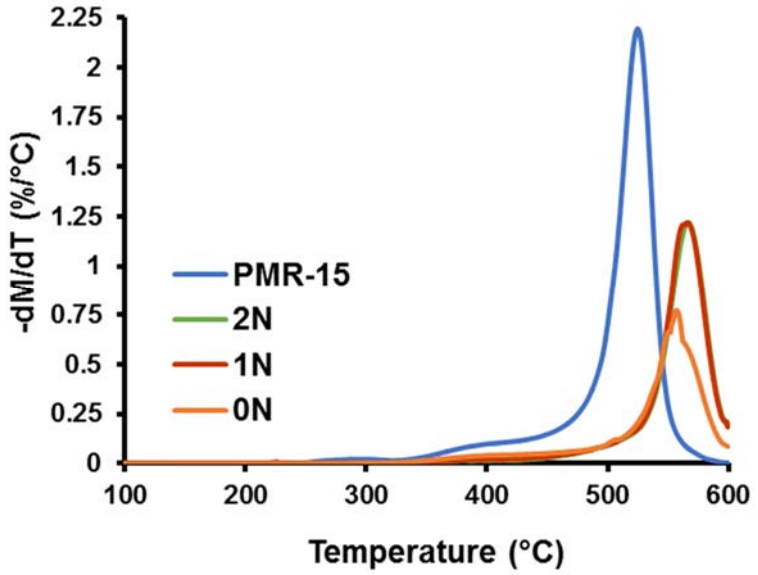

Figure 16. The derivative of mass loss as a function of temperature, measured by TGA at 1 °C/minute air. The peaks designate mass loss events.

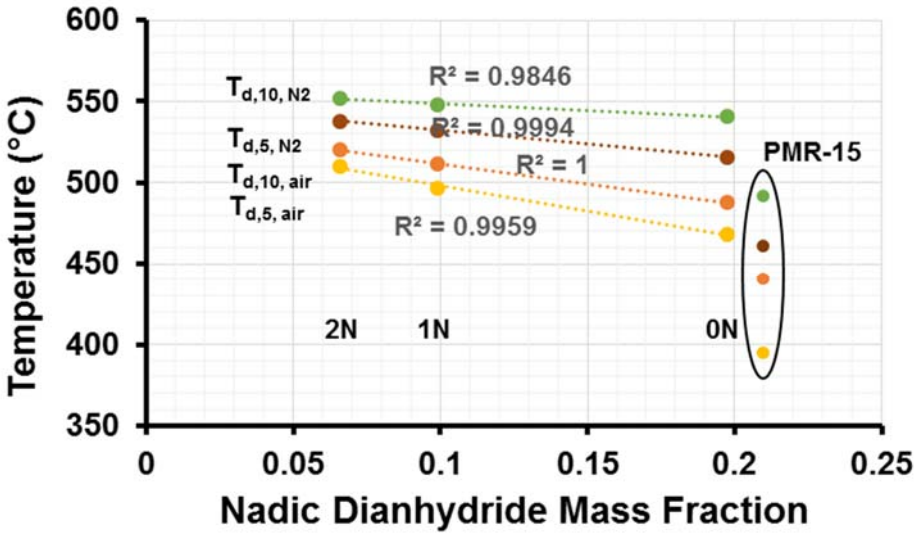

Figure 17. Temperatures at which 5 and 10 percent mass losses (Td,5 and Td,10) occur in both nitrogen and air, plotted against nadic dianhydride mass fraction.

DSC experimentation revealed little to no cure reaction of the nadic end group at 250 °C for sufficiently long periods of time, therefore the rheological characteristics of PMR-15 in comparison with the POSS-containing oligoimides were measured at this temperature via parallel plate oscillatory shear. At a gap spacing of 0.7-0.8 mm, the angular frequency was systematically increased at a strain amplitude of 1%. This complex rheological experiment enables resolution of the storage and loss moduli, which are used to calculate complex viscosity, plotted in Figure 18. PMR-15 exhibits the highest complex viscosity profile at low frequency of 10^9 cP. Replacement

of MDA with POSS results in over an order of magnitude lower complex viscosity as evidenced by the profile for the 2N material. For the POSS-containing oligoimides, complex viscosity decreases with molecular weight. The viscosity dependence of the 1N and 2N materials is relatively frequency insensitive in comparison with PMR-15 (having higher interactions between oligomer chains) and 0N (very low level of interactions). It is evident that POSS reduces inter-oligomeric contact, acting to increase free volume in the liquid (and likely solid) states.

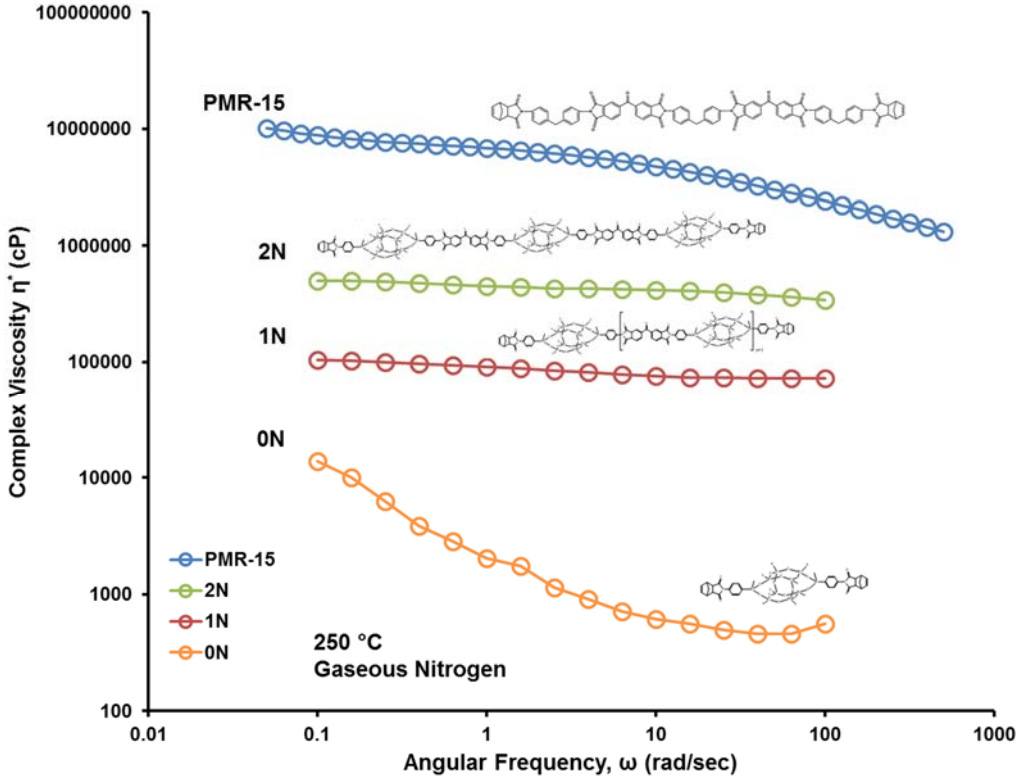

Figure 18. Complex viscosity as a function of angular frequency at 250 °C, a gap spacing of 0.7-0.8 mm, and oscillatory strain of 1%.

Further analysis may be conducted on the storage and loss moduli profiles. A log-log plot of storage (G′) and loss (G″) moduli as a function of angular frequency is shown in Figure 19. In all cases, the magnitude of the loss moduli are greater than those of their storage counterparts, and no crossover frequencies are witnessed at this temperature, indicating that the oligoimides are more viscous than elastic under these conditions at all frequencies. The slopes for both G′ and G″ are close to 1 for all of the materials excluding 0N suggesting relatively low interactions between oligomer chains. 0N demonstrates a slope of 2 in G′ at low frequency, tailing toward lower slope at higher frequency suggesting rigid rod-like behavior. The elasticity of 0N is very low in comparison with the other oligoimides, attributed to its short chain length and expectedly narrow molecular weight distribution.

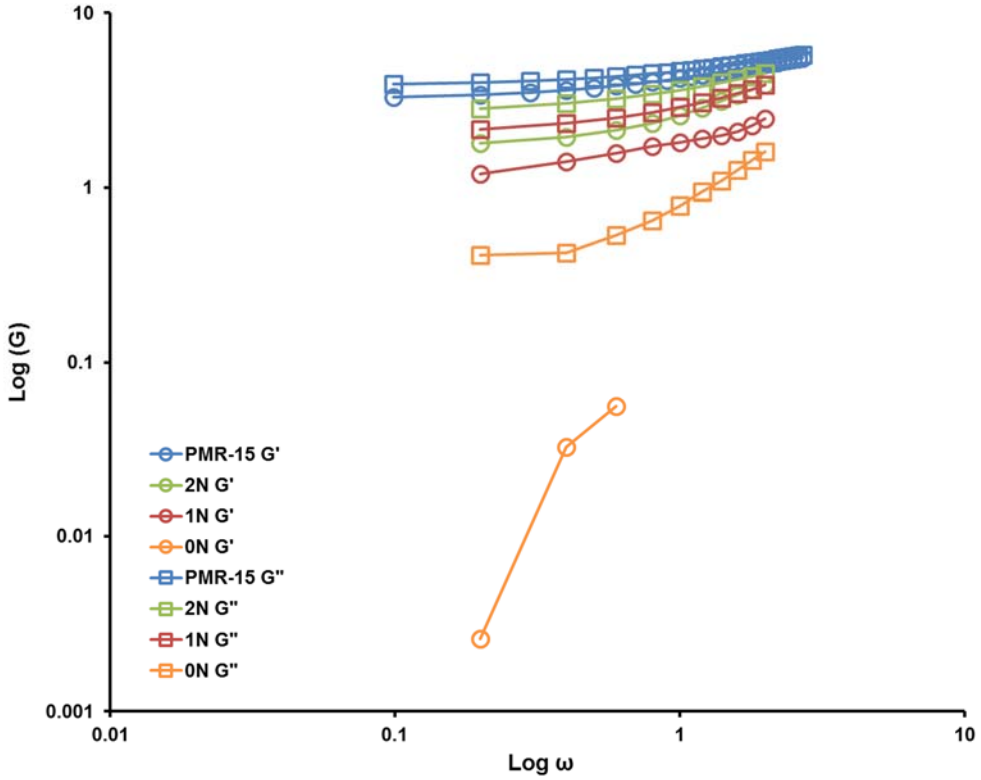

Figure 19. Log-log plot of storage (G′) and loss (G″) moduli as a function of log angular frequency at 250 °C.

The second phase of resin characterization required compression molded disks having dimensions of 12mm in diameter and 1-2mm thick. To fabricate these specimens, steel tooling comprised of a cylindrical housing with a piston and platform was charged with approximately 0.4 g of amic acid or imidized oligomeric powder, assembled, and situated between the platens of a heated press. A vacuum line was also connected to the mold to assist with removal of volatiles emanating from imidization and resin cure. Temperature and pressure were programmed and carefully controlled during the densification and curing process. For PMR-15, standard processing protocol entails heating the material under minimal pressure and full vacuum to ~280 °C at which time ~200 psi are applied to densify the part. The temperature is raised to 315 °C where pressure is held for 1.5-2 hours, after which the mold is cooled and the disk can be removed from the mold. Photographs of the compression mold, heated press, and a cured disk of PMR-15 are shown in Figure 20. Although the processing of PMR-15 and 2N were comparatively trivial experiences, disk fabrication of 1N and particularly 0N were difficult due to their much lower viscosities at the processing temperatures of interest. In attempts replicating the process for PMR-15, the oligomers flowed out of the mold very quickly during pressurization, exacerbated by the observation that POSS-containing materials tend to wick steel. Any residual cured material left inside of the mold was typically found to be full of voids. To mitigate these issues, staging of the POSS-containing materials in the rheometer was conducted prior to compression molding.

Figure 20. Photographs of compression mold tooling, heated press, and a cured disk of neat PMR-15.

During staging, the material of interest is cured to a certain extent to raise its viscosity, but not to the extent that it will no longer flow. Viscosity development was measured using the rheometer. An example of this process is graphically depicted in Figure 21 for 0N. As it was observed that PMR-15 did not leak out of the mold during pressurization, a non-isothermal viscosity profile was measured to resolve its lowest viscosity, which was found to be ~10^6 cP. In contrast, the viscosity of 0N at its lowest point is ~6000 cP. 0N was ramped non-isothermally in the rheometer and its curing reaction commenced at 280 °C. The reaction was allowed to proceed until the material's viscosity reached 10^6 cP. At that point, the material was quenched to prevent further reaction and isolated. Staged resin was then successfully utilized to compression mold disks with minimal leakage.

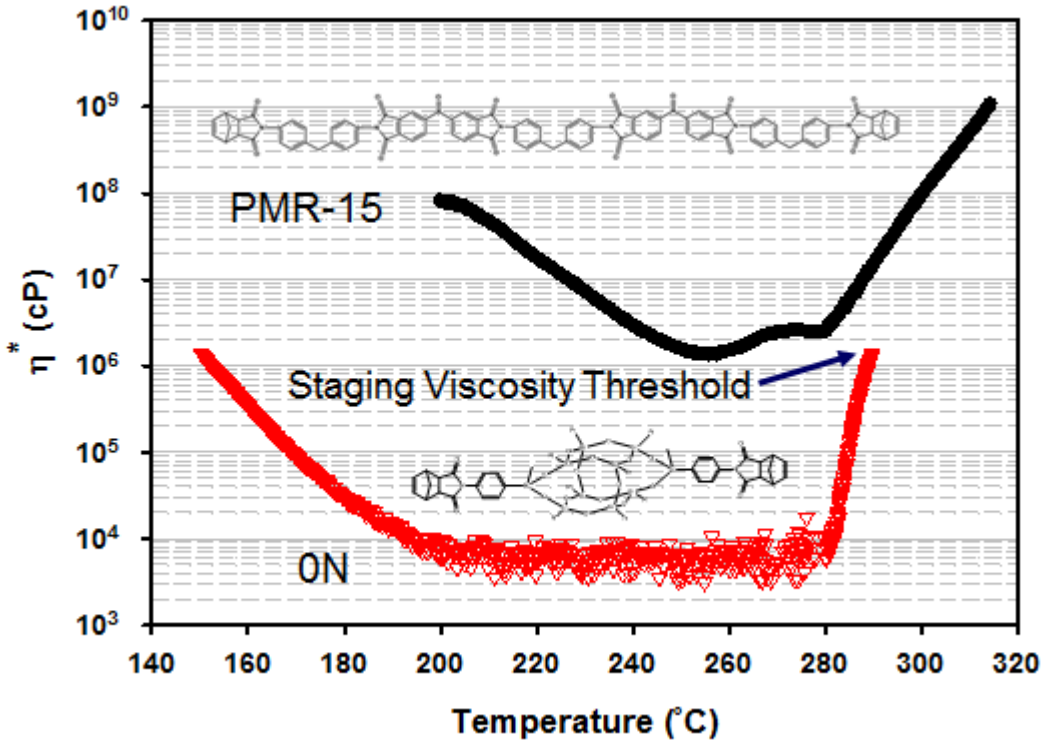

Figure 21. Complex viscosity profiles of PMR-15 and 0N during non-isothermal temperature sweeps during oscillatory shear.

Also of note in examination of the complex viscosity profiles in Figure 21 is the apparent kinetics of the nadic crosslinking reaction. The slope of viscosity development beginning at 280 °C is much higher than that of PMR-15. This is attributed to the lower viscosity of 0N promoting molecular mobility in addition to the higher concentration of nadic end groups. As FTIR is not a feasible technique to measure nadic crosslinking kinetics, as discussed previously, a rheological technique such as this is useful in quantifying reaction rates and viscosity development during thermoset cure, and more valuably feeds into process development.

Using staging techniques, disks were successfully fabricated from all of the oligomers. Characterization activities on these specimens were performed on one disk of each composition including density, viscoelastic characterization by TMA (non-destructive), moisture uptake and diffusion (non-destructive), followed lastly by thermo-oxidative (TOS) stability (destructive).

The average densities of the cured oligoimide networks, resulting from three measurements, are tabulated below (Table 7). PMR-15 exhibits the highest density while the POSS-containing materials have values that correlate with POSS mass fraction. With increasing POSS content, density decreases, in spite of assumed increased crosslink density resulting from the shortened chain lengths in 1N and 0N, in comparison with 2N. This finding expectedly suggests that POSS dominates network architecture due to the large volume that it occupies in relation to BTDA and NA. POSS likely reduces the degrees of freedom of curing networks, drives increases in free volume, and reduces the number of conformational states that a network could self- assemble to due to its size and inflexibility. This hypothesis may be supported by the low standard deviation in measured density for 0N.

Table 7. Average densities resulting from three measurements on each cured disk. Values were measured by immersion in methanol on a balance.

Material	Average Density (g/cm^3)	Standard Deviation
PMR-15	1.284	0.0121
2N	1.268	0.0184
1N	1.253	0.0140
0N	1.238	0.0028

The solid-state viscoelastic properties of the cured networks were examined by modulated TMA. The contact probe was oscillated at a frequency of 0.05 Hz during temperature scans at 5°C/minute. Analagous to complex melt rheology, the material response to oscillating compressive force can be readily decoupled into elastic and loss moduli, all while thermal expansion is measured. By this method, a material's glass transition can be ascertained through treatment of four distinct data sets: onset of drop in storage modulus (G′), the observance of a peak in the loss modulus (G″), peaks in tan delta (δ), and the onset of a change in slope of the dimension change (coefficient of thermal expansion, or CTE) quantifying linear expansion during heating and contraction during cooling. The order of occurrence of transitions generally follows the trend $T_{g,CTE} < T_{g,G'} < T_{g,G''} < T_{g,\delta}$. From a system engineering perspective, $T_{g,G'}$ is most critical as this reflects losses in composite resin elasticity that could precipitate structural failure. In terms of general rules, cured networks of high cross-link density exhibit lower coefficients of expansion,

lower values for tan delta due to elasticity dominance, and more shallow steps to the rubbery plateau in the post-transitional state.

The datasets for these properties are plotted in Figure 22 a-d, respectively, after pre-heating the disks in-situ to 350 °C to baseline their thermal histories and to promote residual cure, followed by cooling to 50 °C in preparation for the final sweep. To preface data analysis, 2N, 1N, and 0N all feature the same weight fraction of POSS (0.80), but differ in average chain length and POSS volume conentration, affecting the distance between cross-link junctions in the cured state. First, it is apparent that all datasets converge to PMR-15 demonstrating the highest T_g (quantified in Table 8) no matter what form of measurement. Co-oligomerization with POSS clearly lowers T_g, successfully offset to some degree by shortening oligomer chain length. Also common amongst the POSS family of oligomers is a weak relaxation event activated just above 200 °C, possibly attributed to POSS cage excitation. POSS also generally increases CTE, especially after the transition from a glassy to rubbery state. All of the cured networks demonstrate δ below 0.2 except in the transition region, indicative of highly crosslinked thermoset networks. δ signals for the POSS materials are slightly higher than PMR-15, a signature of more dampening character, likely due to their reduced densities, higher degees of free volume, and mild translational capabilty of the POSS cage itself. The 1N cured network exhibits somewhat anomolous behavior with a less steep transition into the rubbery plateau and lower CTE in the pre-transition state, as well as lower δ in the transition region. These results suggest a possibly higher degree of cure, perhaps due to a balance in thermal induced molecular mobility and optimized oligomer segment length, but steadfast conclusions cannot be drawn from one set of experiments. This behavior could be due to experimental error of specimen imperfections in the contact surface, etc.

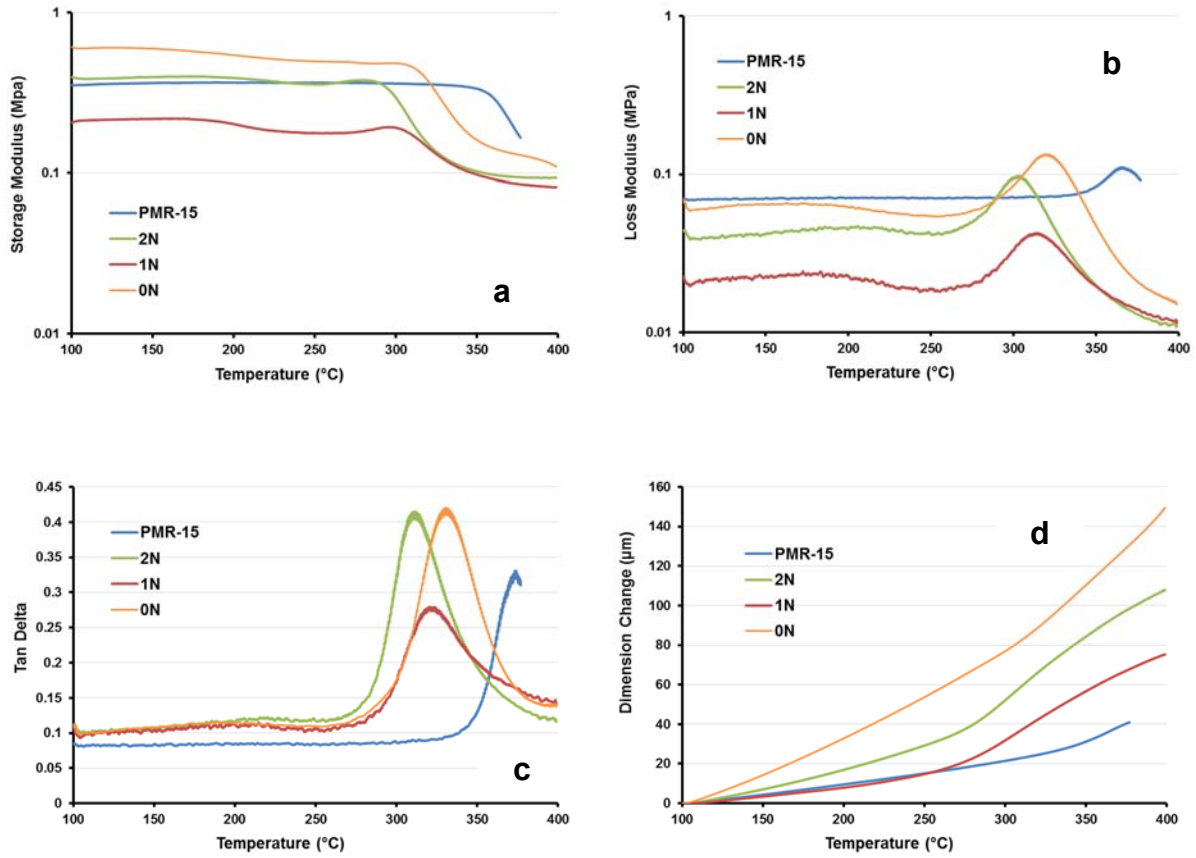

Figure 22. Plots of storage modulus, G′ (a), loss modulus, G″ (b), tan delta, δ (c), and coefficent of thermal expansion, CTE, (d).

Table 8. Quantified values of the glass transition temperature (T_g) as measured from the salient characteristics of storage modulus (G′), loss modulus (G″), tan delta (δ), and coefficent of thermal expansion (CTE).

	Tg (°C)			
	Storage Modulus	Loss Modulus	Tan Delta	Dimension Change
PMR-15	343	366	374	319
2N	288	303	312	274
1N	301	315	321	265
0N	304	315	326	293

Water diffusion and saturated uptake in composites and composite resin systems is an issue of practical significance due to associated effects pertaining to property degradation as well as rapid release during structure heating leading to blistering and delamination. In some cases, property degradation is irreversible. Polyimides are especially susceptible due to their highly polar

character. POSS has been shown to reduce water affinity in other polyimide-based thermoplastic [27] and thermoset systems [22]. To determine if POSS provides water resistance to the materials of this study, the cured disks utilized for TMA were immersed in boiling deionized water and their masses were measured systematically until saturation was observed. The resulting basic raw data is plotted in Figure 23. The behavior of the POSS-containing materials is remarkably different than that of PMR-15. Diffusion is a much more gradual process for PMR-15, reaching saturation at approximately 24 hours, with a mass gain of 4.3%. The POSS materials reach saturation within a single hour, but the mass gain is 4 times less, with 2N gaining 0.93%, 1N 1.1%, and 0N 1.25%, highlighted for comparison in Figure 24. Saturated mass gain correlates to density amongst the POSS materials in that 0N takes up the most water, albeit a marginal difference. Although it may be concluded that more porous networks such as that of 0N canaccommodate more water molecules for the POSS polyimides, this does not hold true when examining PMR-15, which exhibits the lowest density of all but by far the highest mass gain. The imide and carbonyl groups of PMR-15 are polar and are known to participate in inter-chain Van der Waals intractions with each other (termed charge transfer complexing, or CTC interactions). These sites have been shown to have a propensity for hydrogen bonding with water molecules [28]. During the process of water infiltration and hydrogen bonding, polyimides have been shown to expand through long range translational chain motion processes that allow for more water to be accomodated, forming dimers or greater degrees of coalescence. Although this phenomena is likely to explain the behavior of PMR-15, it does not appear to hold for the POSS-containing networks due to the rapidity of water ingress to saturation. The data suggests that water molecules enter the POSS-containing networks very quickly to occupy available volume, rather than long diffusion-dominated processes. This hypothesis is supported by the observance of marginal differences in saturated uptake based on cured network density. It is further postulated that water molecules cannot generally hydrogen bond with carbonyl and imide groups in the POSS-containing materials as they may be shielded by the relatively large cage structure and peripheral phenyl groups. Although the POSS-containing networks are less dense than PMR-15, the free volume introduced by POSS may not be largely accessible to water molecules, and this may be largely due to the aromatic peripheral groups. It would be informative to understand the state of the networks and how they are affected by POSS, which could be the subject of thermoset cure modeling, but was beyond the scope of this effort.

Attempts were made to quantify the diffusion coefficients for the subject cured polyimides using the Fickian diffusion model [29], applying a least squares minimization strategy. These results are plotted in Figure 25, where normalized sorption functions (G(t)) are plotted against $\sqrt{t}$ divided by specimen thickness, h. Very good agreement for PMR-15 is found, and its diffusion coefficient is calculated to be 3×10^{-5} mm^2/s. Significant scatter in the data for the POSS-containing materials exists, and this is in part due to the imperfect disks in terms of uneven dimensions that were fabricated and used for this testing. As discussed earlier, cured disks of the POSS-containing oligomers were difficult to process resulting in some geometric irregularities. Nonetheless, attempts were made to quantify their water diffusion coefficients and these results are depicted in Table 9. The diffusion coefficients for 2N and 1N are estimated to be 1×10^{-4} and 1.7×10^{-4} mm^2/s, significantly higher than PMR-15 and again showing some dependence on network density. The diffusion coefficient for 0N was found to be only slightly higher than that of PMR-15, possibly due to more difficult diffusion paths for water molecules complicated by increased crosslink density and POSS volume/peripheral phenyl group concentration.

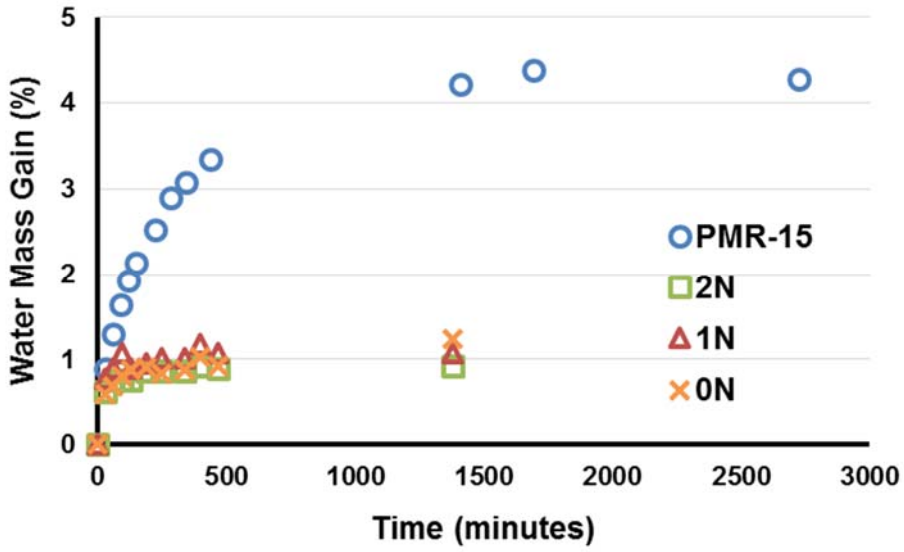

Figure 23. Moisture diffusion profiles for the cured polyimide networks during boiling water immersion.

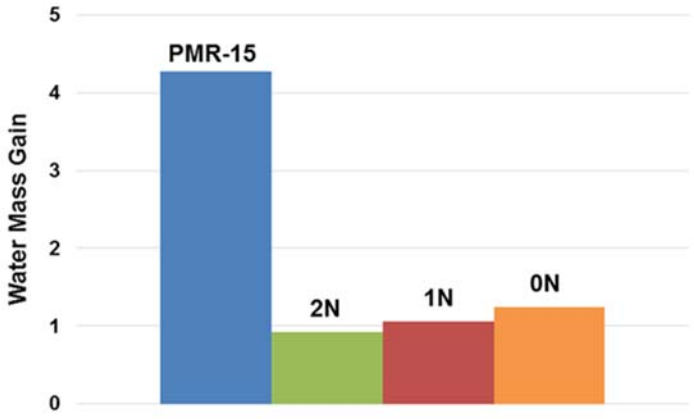

Figure 24. Bargraph chart comparing the saturated moisture uptake in the cured polyimide networks after boiling water immersion.

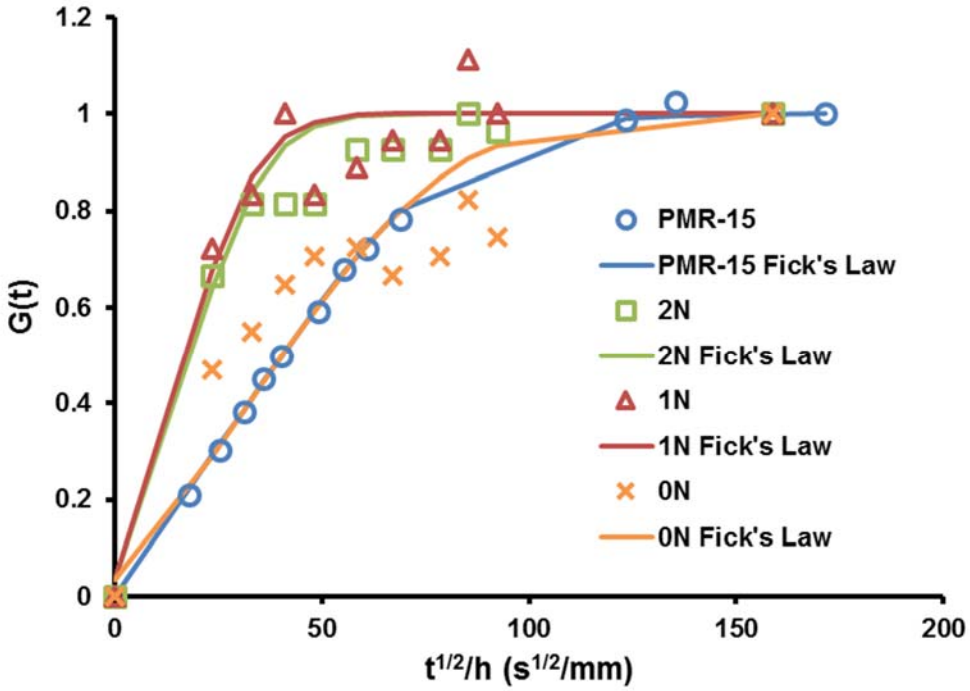

Figure 25. Boiling water sorption functions G(t) for the cured polyimide networks, based on immersion.

Table 9. Cured densities, water diffusion coefficients (D), and saturated water mass gain. The latter two properties were determined from boiling water immersion studies.

	Density (g/cm^3)	D (mm^2/s)	Water Mass Gain (%)
PMR-15	1.284	0.000029	4.27
2N	1.268	0.0001	0.93
1N	1.253	0.00017	1.07
0N	1.238	0.00003	1.24

A benefit from increased moisture diffusion coefficients is that diffused water molecules in composite structures can more easily escape during rapid heating with less probability of damaging the structure. In essence, POSS appears to render more breathable resin network structures, but does not result in increased saturated moisture content, but rather a resistance to significantly higher water occupation as seen with PMR-15. Unfortunately, if water molecules can more readily penetrate a network, so can oxygen during exposure of composites to elevated service temperatures. To quantify long-term thermo-oxidative stability (TOS), the cured disks were dried after the boiling water immersion studies back to their equilibrium masses. The disks were situated on an aluminum mesh positioned on a graphite boat and inserted into a tube furnace with flowing high purity air at a controlled rate. The temperature was set at 316 °C to accelerate aging processes. The specimens were periodically removed from the furnace and weighed to determine their weight loss. The results are plotted in Figure 26. For each data set, three regimes of mass loss can be distinguished: 1) initial non-linear accelerated loss, 2) linear gradual loss, and 3) slowed loss at long exposure times. The slopes of the linear portions of the mass loss data sets

are readily quantified to be PMR-15 (3×10^{-3} %/hr), 2N (2.2×10^{-3} %/hr), 1N (2.6×10^{-3} %/hr), and 0N (7.8×10^{-3} %/hr). The mass loss rate of 2N and 1N are lower than PMR-15 in the linear regime, while that of 0N is higher. These rates likely stem from nadic crosslink concentration in the networks, as described in the TGA data analysis section, as 2N>1N>0N in terms of relative stability.

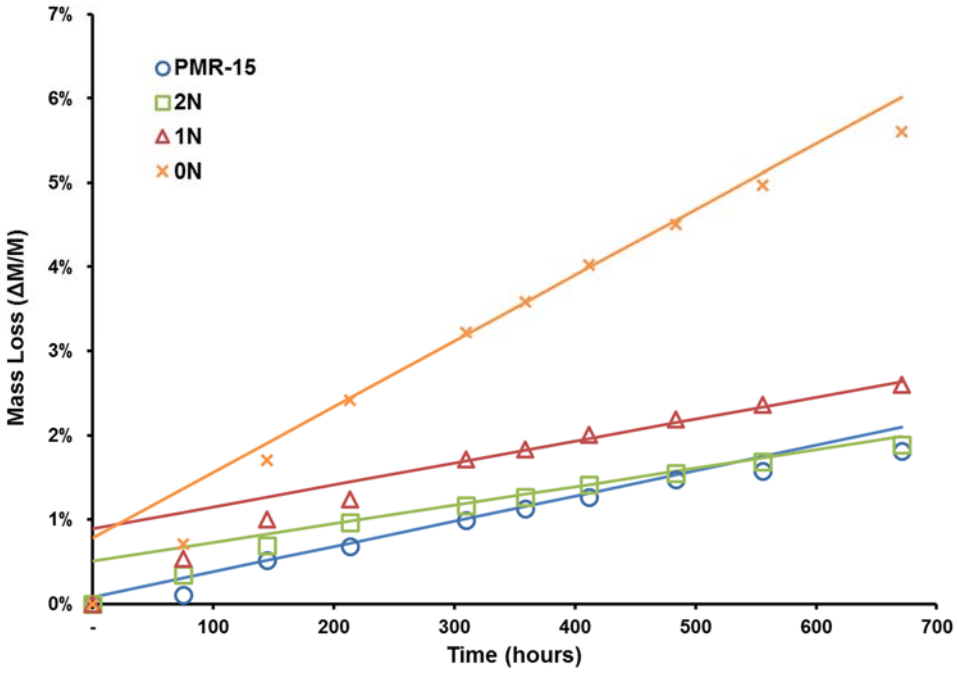

Figure 26. Mass loss profiles for the cured polyimide networks as a function of exposure time to 316 °C and flowing air conditions precisely controlled in a tube furnace.

Approach 2 for oligomer synthesis and characterization was briefly explored, entailing synthesis of oligomers from PA, p-PDA, POSS, and NA. p-PDA and PA, when copolymerized, are known to produce an intractable (unprocessable) polymer with exceptional thermal stability. In the context of the rheological effects in terms of enhanced flow characteristics witnessed when POSS is co-oligomerized, it was hoped that the combination of these monomers would afford a thermoset with good processability yet high cured T_g and thermal stability. PA (phthalic dianhydride) was not on-hand, therefore pyromellitic dianhydride (PMDA), known for its use in Kapton, was used instead. An oligomer equivalent in terms of PMR-15 was targeted for synthesis ($PMDA_2$-p-PDA_1-$POSS_2$-NA_2). During synthesis, fractionization occurred, presumably a result of the differences in reactivity of the two aniline monomers (PMDA-p-PDA-NA would likely crash out of solution). The fractionated solution was filtered into a filtrate which required further isolation and a filtrant. The former was suspected to be some form of PMDA-POSS-NA as it remained soluble in THF, while the filtrant was suspected to be a form of PMDA-p-PDA-NA. The two fractions were separately analyzed by DSC. The filtrant did not exhibit an uncured or cured T_g, while the filtrate had an uncured T_g of 113 °C and a cured T_g of 329 °C, very similar to PMR-15 (333 °C). This approach was not further pursued due to lack of resources, but with this result

in mind, oligomers of the following architectures may be pursued at a later date: $PMDA_2$-$POSS_3$-NA_2, PA_2-$POSS_3$-NA_2, $PMDA_1$-$POSS_2$-NA_2, and PA_1-$POSS_2$-NA_2.

Resin selection down to one candidate for scaleup to facilitate composite fabrication and testing was made based on the data collected during Task 3. The results are summarized in Table 10. Properties that exceeded threshold requirements are color coded as green while those that were measured to be deficient are red. Areas where the POSS-containing materials fell short were in long-term TOS, with the exception of 2N, again because of increased nadic end group concentration in 1N and 0N, and cured T_g. Although the literature value for PMR-15 that is not post-cured is 299 °C, this value was not used as a baseline for comparison because 343 °C was measured. Based on these results, the 0N material was chosen for scaleup despite having poorer TOS performance. This oligomer was chosen because it features the highest T_g with the weakest relaxation. Risks identified with this choice were oligomer cost based on market pricing of the POSS tetrol feedstock precursor, the potential for poor composite mechanical properties due to its presumably high crosslink density, and poor adhesion between carbon fiber and the POSS-dominated resin matrix in composite form. Nonetheless, this choice was made in an attempt to counter reductions in cured T_g resulting from POSS co-oligomerization. A 200 g batch was synthesized and was characterized by NMR as well as by DSC, and the material was considered to be equivalent to that synthesized from smaller batches.

Table 10. Key properties of PMR-15 (literature, **measured**) in comparison with those of 2N, 1N, and 0N. This data was used to select a resin for synthesis scaleup.

Property	**PMR-15**	**2N**	**1N**	**0N**
Zero Shear Viscosity (@ 150 °C, P)	1.16×10^6	-	-	-
Zero Shear Viscosity (@ 250 °C, P)	**100688**	**4978**	**1047**	**139**
T_g (°C, no postcure) – measured by TMA (Storage Modulus)	299 (**343**)	**288**	**301**	**304**
T_g (°C, postcured in air at 316 °C for 24 hrs)	333	-	-	-
Weight Loss (% @ 316 °C/400 hrs in air)	1.88 (**1.3**)	**1.4**	**1.9**	**3.9**
Weight Loss (% @ 316 °C/500 hrs in air)	4.97 (**1.6**)	**1.6**	**2.2**	**4.7**
5% Weight Loss Temperature (°C, 1 °C/min ramp, N_2 purge	440 (461)	**520**	**512**	**488**
Coefficient of Thermal Expansion (μm/mm·°C)	55 (**121**)	**-**	**-**	**-**
Moisture Uptake (100 hrs, 80 °C/80 RH)	4.0 (1.6)	**0.8**	**1.1**	**0.8**

Task 4: Composite Fabrication

The general composite fabrication strategy for PMR-15 is visually represented in Figure 27. A solution of PMR-15 oligoamic acid was first made by dissolving powder in methanol. The resultant solution was painted onto pre-cut plies of IM7 4 harness satin weave fabric, and dried in an oven at 60 °C for an hour to drive off most of the methanol, leaving some behind in the pre-preg to provide tack and drape characteristics. Composite fabrication entailed symmetric layup of, from the mold surface inward: (1) Teflon release film, (2) woven fiberglass bleeder, (3) perforated Teflon film, sequenced pre-preg layup, (4) perforated Teflon film, (5) woven fiberglass bleeder, and (6) Teflon release film, inside the cavity of a picture frame-type steel mold. 14 plies of pre-preg were stacked to render a composite that was approximately 0.1 inches in thickness after consolidation. The mold pressure intensifying piston was placed on top of the layup and the assembly was placed between the platens of a heated press. The commercial cure cycle for PMR-15 was implemented. After cool down, the mold was disassembled resulting in a cured laminate that was sectioned into specimens for mechanical testing. A microscopy image of the cross-section of PMR-15 is shown also in Figure 27, demonstrating excellent consolidation and low void content.

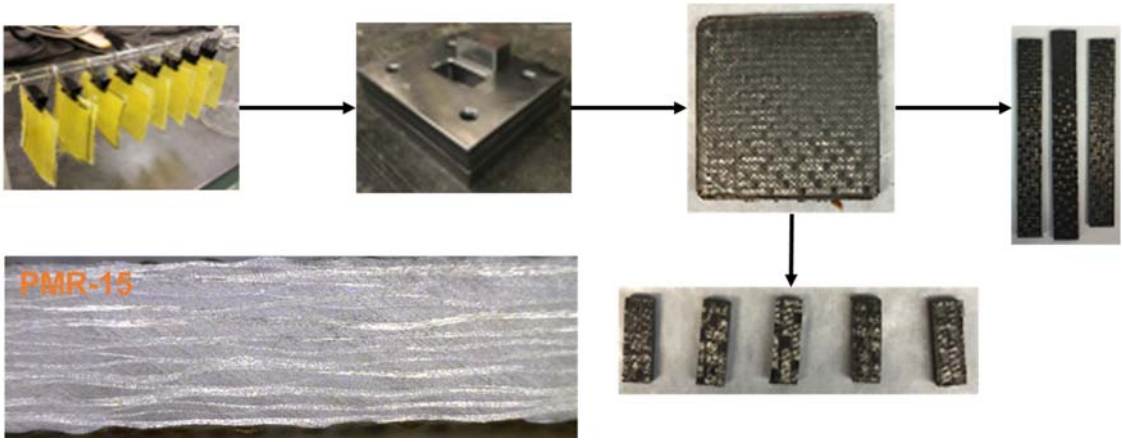

Figure 27. Visual schematic of the process for PMR-15 composite fabrication, and a cross-sectional image of resultant composite demonstrating good consoliation and low void content.

Because 0N oligoamic acid is insoluble in methanol, the industry preferred solvent for PMR processes, pre-preg would have had to have been made using THF as the carrier solvent. Discussions with pre-preg manufacturers (i.e. Maverick and Renegade Composites) and end users such as Boeing and Lockheed Martin indicated that this prospect was a viable possibility, as THF is considered non-toxic. However, this was viewed as an opportunity to showcase the low viscosity of the oligomer in a process mimicking resin transfer molding, or RTM, without the use of solvent, the environmentally preferred option. From an AF perspective, RTM processes are often used in the manufacture of aerospace components including several for F-22 and F-35, due to its relative simplicity and lower cost in comparison with pre-preg layup. In RTM, a textile preform is placed into a mold or die, and densified through contact pressurization. Thermosetting resin is then flowed through the preform, backed by pressure and often assisted by vacuum, until

complete saturation, after which the composite is cured through the application of heat. This process reduces environmental footprint due to lower accumulated waste and non-use of solvent, and facilitates the manufacture of parts with less voids, smoother surface finishes, and more complex geometries than pre-preg processing affords. Resin viscosity requirements for RTM are typically below 1000 cP such that sufficient flow through the preform can occur. This is easy to achieve with epoxies, acrylates, and polyesters, but these resin systems typically feature low use temperature capabilities. High temperature resin systems, especially polyimides, generally have very high viscosities, even at temperatures above 200 °C, precluding their use in RTM processes. Bismaleimides (BMIs), offering temperature capability between epoxies and polyimides, in some cases have been specifically tailored at the constituent monomer level to afford viscosities amenable to RTM (most notably Cytec CYCOM 5250-4 RTM). There is a need in the aerospace community for a high temperature service composite resin system that can be RTM processed. The shear rate dependence of viscosity on steady shear of 0N at 250 °C is plotted in Figure 28. Under quiescent conditions, the viscosity of 0N is just above 14000 cP, but rapidly drops to ~1000 cP at 0.1 s^{-1} shear rate. It is therefore possible that 0N could be successfully implemented in an RTM process, albeit at high reservoir temperature.

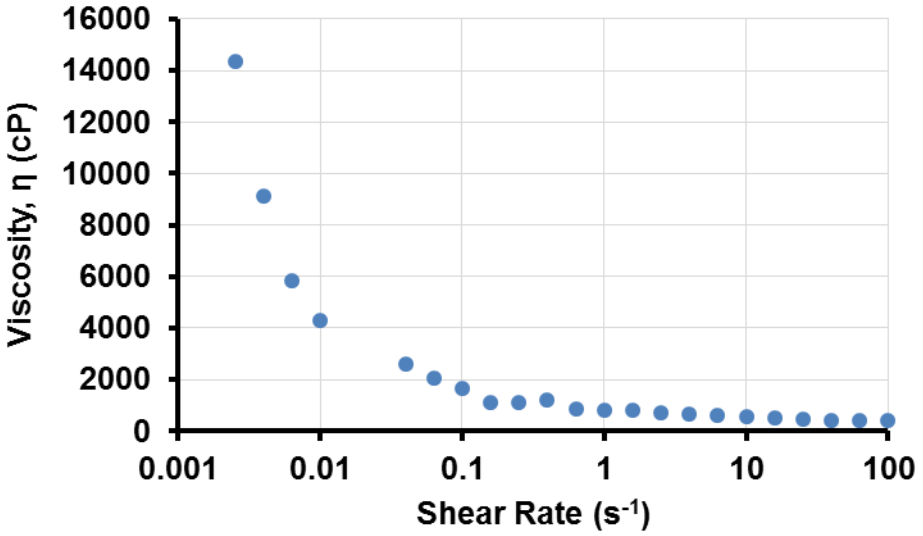

Figure 28. Steady shear rate dependence of the viscosity of 0N at 250 °C.

To demonstrate the potential viability of 0N for the RTM process, the layup procedure utilized for PMR-15 was again followed, but in this case bare IM7 fabric was used and a pre-measured amount of 0N powder was placed between plies 7 and 8, as depicted in Figure 29. The cure process for PMR-15 was again implemented. The resultant part indicated good resin flow into all of the carbon fabric plies, a positive first sign that this resin could be explored in conventional RTM processes. A cross-sectional micrograph of the 0N composite highlights more void content than that fabricated from PMR-15, but probably not to the extent that it is unusable.

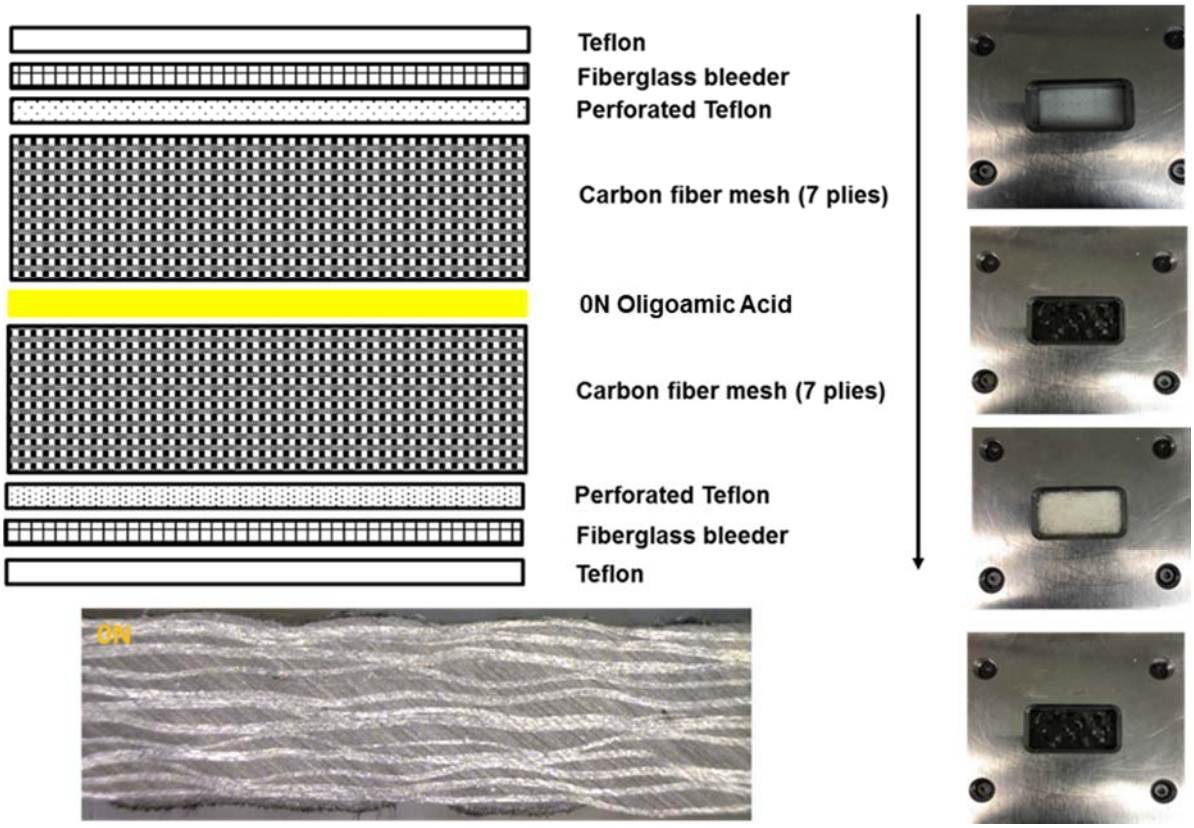

Figure 29. Illustration depicting the layup process for the fabrication of 0N-based composite. Instead of using solvent-containing pre-preg, the resin powder was placed in between the carbon fabric stacked ply sequence and the low viscosity of the resin was relied upon to infiltrate the entire preform, similar to an RTM process.

To quantify resin, carbon fiber, and void contents in the composite panels, digestion methods were utilized. The PMR-15 composite resin matrix was readily digested in conventional sulfuric acid over the period of one day. The 0N composite, on the other hand, was not affected by acid whatsoever. POSS is known to be acid resistant, but this finding was slightly surprising due to the strength of the acid used. With the knowledge that POSS is affected by base, sections of 0N composite were soaked in a 55 weight percent solute KOH solution. In one week, the matrix resin appeared to be completely digested. After matrix resin digestion, hydrogen peroxide is added to decompose the resin digested products, and the fiber is isolated, washed, and weighed. Based on the initial volume and mass of the test section, the known densities of the resin and fiber, and the measured fiber mass after digestion, the resin and void contents can be readily calculated. The quantitative results of digestion are tabulated in the inset of Figure 30. For PMR-15, the resin and void contents were measured to be 29.8 and 1.9%, respectively, while that of 0N were found to be 28.7 and 3.5%, respectively. Due to the similarities in resin content between the two different composite materials, it was concluded that the process developed for 0N was successful. Although the void content of the 0N was almost twice that of PMR-15, the void constituency was deemed low enough for useful mechanical property evaluation. Void content could likely be reduced through slight manipulation of the cure cycle for 0N.

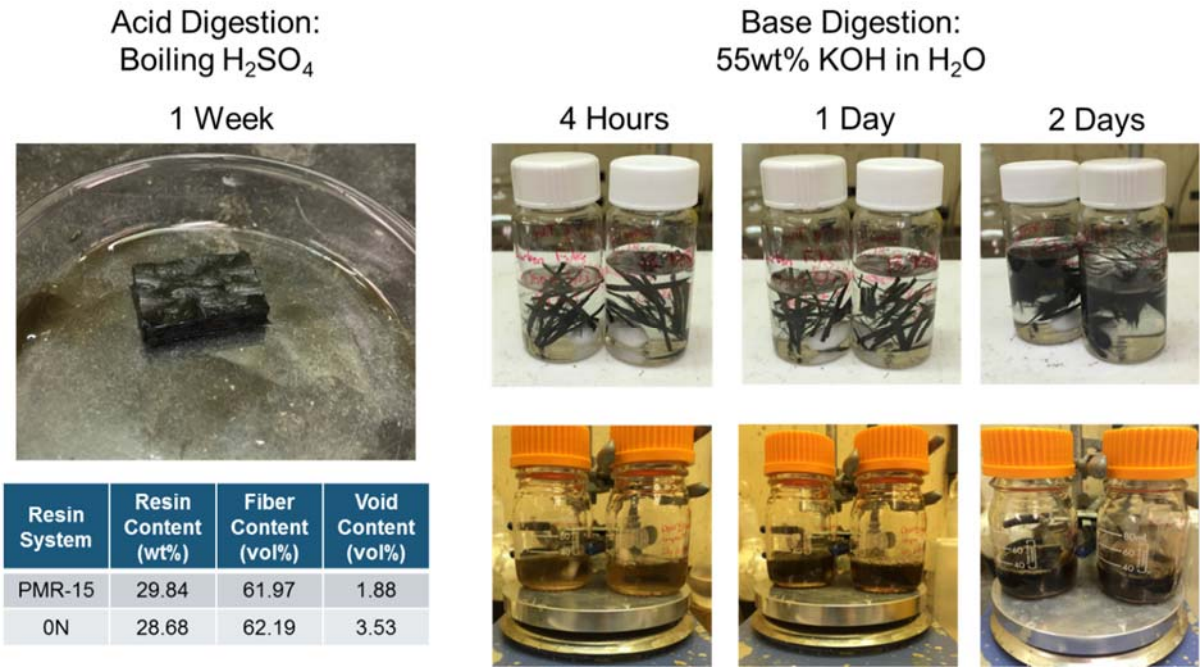

Resin System	Resin Content (wt%)	Fiber Content (vol%)	Void Content (vol%)
PMR-15	29.84	61.97	1.88
0N	28.68	62.19	3.53

Figure 30. Time lapsed photographs of the digestion processes for the PMR-15 and 0N/IM7-4HSW-GP composites to ascertain constituent ratios. The quantitative results are shown in the inset table.

Task 5: Composite Characterization

Although a variety of types of composite mechanical tests could have been chosen for this task, only tests that focused on the key risks associated with POSS-containing resin systems were chosen for examination. In all likelihood, if the tensile properties were chosen to be measured for comparison, for instance, this test would not have provided insight on the key deficiencies of this experimental resin system. Two key risks were identified for the 0N resin system: adhesion of this resin to carbon fiber as the primary constituent is POSS which might be expected to have a greater affinity for glass over carbon, and reduced toughness of the resin system due its relatively high crosslink density, which was implemented in an attempt to offset reduced T_g. Therefore, ASTMs D 2344 (short beam or interlaminar shear) and D 7264 (flexural strength) were chosen to key in on potential weaknesses of the 0N resin system. The basic testing architectures of 7264 and 2344 are shown in Figures 31 and 32, respectively. For flexural strength testing, a specimen ratio of 32:1 L/h was used as recommended and for interlaminar shear strength testing, the L/h ratio was 4:1. Three samples of PMR-15 and 0N composite were tested to failure by ASTM D 7264, the results of which are shown in Table 11. The average flexural strength for PMR-15/IM7-4HSW-GP is ~1850 MPa, much higher than the literature value of 1082 MPa with T650-35, because the latter is a unidirectional textile tape rather than a woven fabric, the latter providing greater flexural resistance. The average flexural strength of the 0N/IM7-4HSW-GP composite is 405 MPa, 78% less than that of its PMR-15 counterpart. The most significant contribution to this drastic reduction in flexural strength is crosslink density of the resin matrix. The 0N resin's crosslink density is much higher than that of PMR-15, inducing embrittlement. The interlaminar shear strength (ILSS) determined from short beam shear testing is presented in Table 12. The average ILSS strength of

PMR-15/IM7-4HSW-GP is 77 MPa, while that of 0N/IM7-4HSW-GP is 22 MPa, 71% less. This knockdown is likely attributed to poor adhesion of the 0N resin system to either the GP (epoxy-based) sizing or the carbon fiber itself. This result is worth continued exploration, because POSS has been used by others as an interfacial strength promoting agent between high temperature resin systems and carbon fiber [30]. The failure mechanism of these composite specimens will be examined by microscopy for further insight.

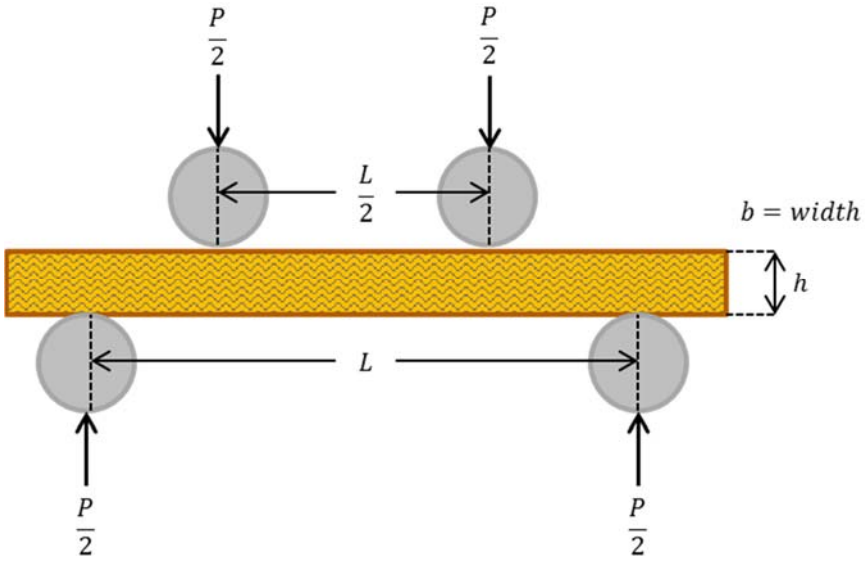

Figure 31. ASTM D 7264 four-point bend testing framework to quantify the flexural strength and modulus of fiber reinforced composite materials.

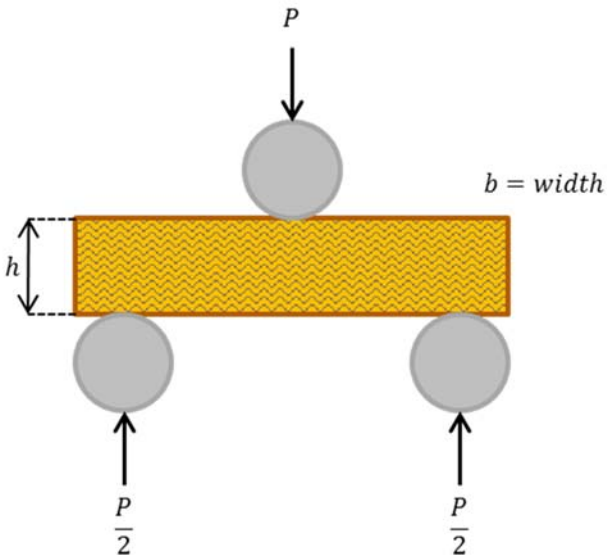

Figure 32. ASTM D 2344 short beam shear testing framework to quantify the interlaminar shear strength properties of fiber reinforced composite materials.

Table 11. Results from flexural testing of PMR-15 and 0N composites containing Hexcel 4 harness satin weave IM7 carbon fiber fabric.

Flexural Strength

Sample	Thickness (h)		Width (b)		Span (L)		**Fracture Stress (σ)**		**Modulus**	
PMR-15	mm	in	mm	in	mm	in	**mpa**	**ksi**	**mpa**	**ksi**
1	2.477	0.1	10.511	0.41	79.4	3.125	1569.2	227.6	435.1	63.1
2	2.675	0.11	9.0856	0.36	85.7	3.375	1601.7	232.3	806.0	116.9
3	2.586	0.1	12.111	0.48	82.6	3.25	2375.2	344.5	1068.2	154.9
						Average	**1848.7**	**268.1**	**769.8**	**111.6**
						StDev	**456.3**	**66.2**	**318.1**	**46.1**

Sample	Thickness (h)		Width (b)		Span (L)		**Fracture Stress (σ)**		**Modulus**	
0N	mm	in	mm	in	mm	in	**mpa**	**ksi**	**mpa**	**ksi**
4	2.591	0.1	13.124	0.52	82.6	3.25	486.8	70.6	342.7	49.7
5	2.875	0.11	13.03	0.51	92.1	3.625	335.1	48.6	538.5	78.1
8	2.634	0.1	12.992	0.51	85.7	3.375	394.4	57.2	612.3	88.8
						Average	**405.4**	**58.8**	**497.8**	**72.2**
						StDev	**76.4**	**11.1**	**139.3**	**20.2**

Table 12. Results from short beam shear testing of PMR-15 and 0N composites containing Hexcel 4 harness satin weave IM7 carbon fiber fabric.

Interlaminar Shear Strength

Sample	Thickness (h)		Width (b)		Max Force (Pm)		**Short Beam Strength (Fsbs)**	
PMR-15	mm	in	mm	in	lbf	N	**ksi**	**mpa**
A	2.6	0.101969	5.4	0.212205	326	1450.048	11.3	77.9
B	2.5	0.098819	5.5	0.216536	323	1436.704	11.3	78.1
C	2.6	0.10315	5.5	0.215354	326	1450.048	11.0	75.9
D	2.6	0.100787	5.3	0.206693	306	1361.088	11.0	76.0
E	2.5	0.098425	5.1	0.201969	293	1303.264	11.1	76.2
						Average	**11.1**	**76.8**
						StDev	**0.2**	**1.1**

Sample	Thickness (h)		Width (b)		Max Force (Pm)		**Short Beam Strength (Fsbs)**	
0N	mm	in	mm	in	lbf	N	**ksi**	**mpa**
A	2.5	0.099606	5.3	0.20748	87	388.3104	3.2	21.8
B	2.5	0.097638	5.2	0.204331	92	406.992	3.4	23.7
C	2.6	0.101181	5.4	0.212599	80	357.1744	2.8	19.3
D	2.5	0.099213	5.1	0.200394	87	386.5312	3.3	22.6
E	2.4	0.096063	5.2	0.202756	91	402.9888	3.5	24.1
						Average	**3.2**	**22.3**
						StDev	**0.3**	**1.9**

The long-term TOS of composites prepared from PMR-15, 0N, and IM7-4HSW-GP was examined at 316 °C, in the same manner as that used for neat resin specimens, and is plotted in Figure 33. Mass loss data was collected to 625 hours. Similar to the resin specimens, the composites demonstrate a period of acceleration of weight loss up to 100 hours, after which a long period of steady linear loss transpires out to ~500 hours, lastly followed by a period of slower loss. In the linear regime, the mass loss rates are readily calculated for comparison. The rate of loss for PMR-15/IM7-4HSW-GP is 1.1×10^{-5} (%/hr), while that of 0N/IM7-4HSW-GP is 4.0×10^{-5}. The rate of mass loss contrast between the composites is 4, while that of the neat resin specimens of PMR-15 and 0N is 3, therefore in compositized form the mass loss in 0N/IM7-4HSW-GP could be exacerbated by increased void content, or poor adhesion between fiber and matrix leaving a path of low electron density for oxygen to attack the composite.

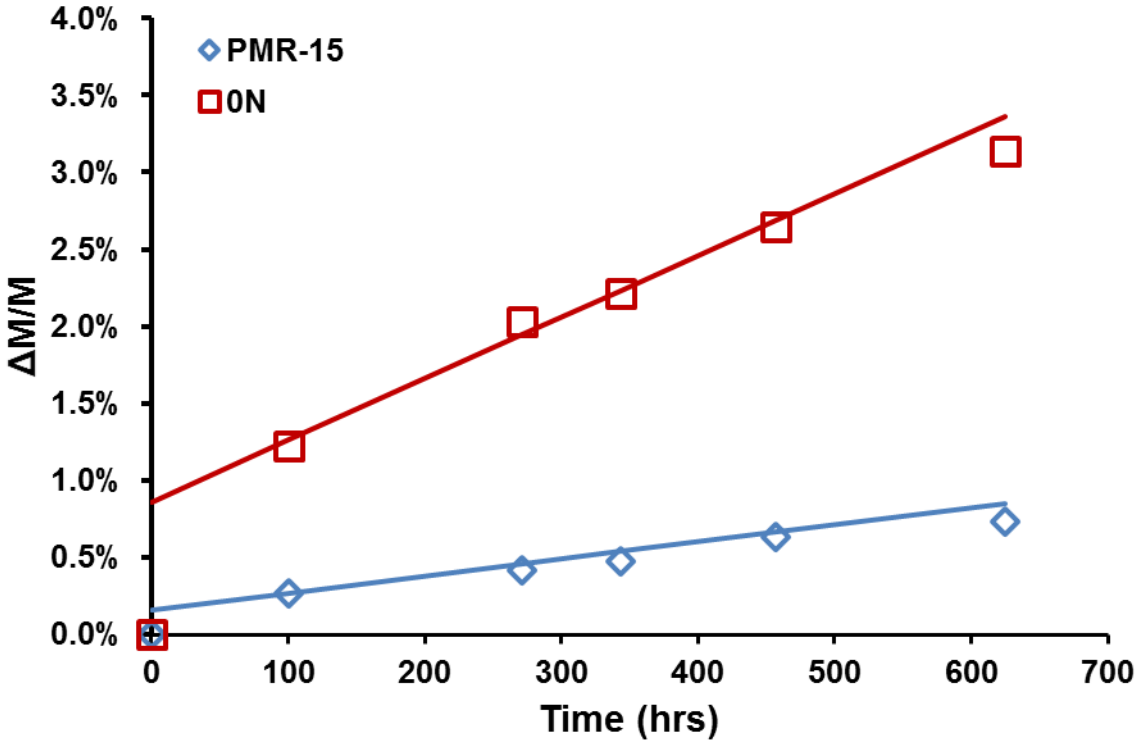

Figure 33. Long-term thermo-oxidative stability mass loss measurements at 316 °C for the PMR-15 and 0N/IM7-4HSW-GP composites.

The cross sections of the composite specimens were imaged using a digital microscope before, during, and after TOS exposure. The pre-test micrographs for PMR-15 and 0N/IM7-4HSW-GP are shown in Figure 34. Few flaws are seen in the PMR-15 composite, while some voids near the surface of the 0N composite are present. Images after 625 hours at 316 °C are presented in Figure 35. For PMR-15, several large in-plane and transverse cracks have manifested, which are known to seriously degrade mechanical properties. Remarkably, the 0N composite exhibits no microcracking or other flaws which may be attributed to TOS aging, despite its

relatively higher mass loss. It is suspected that the POSS cage, due to its slight flexibility, acts to dampen strains in the network caused by thermal, aging, and degradation-induced stresses.

Figure 34. Pre-TOS test optical micrographs for PMR-15/IM7-4HSW-GP (upper) and 0N/ IM7-4HSW-GP (lower) composite cross-sections.

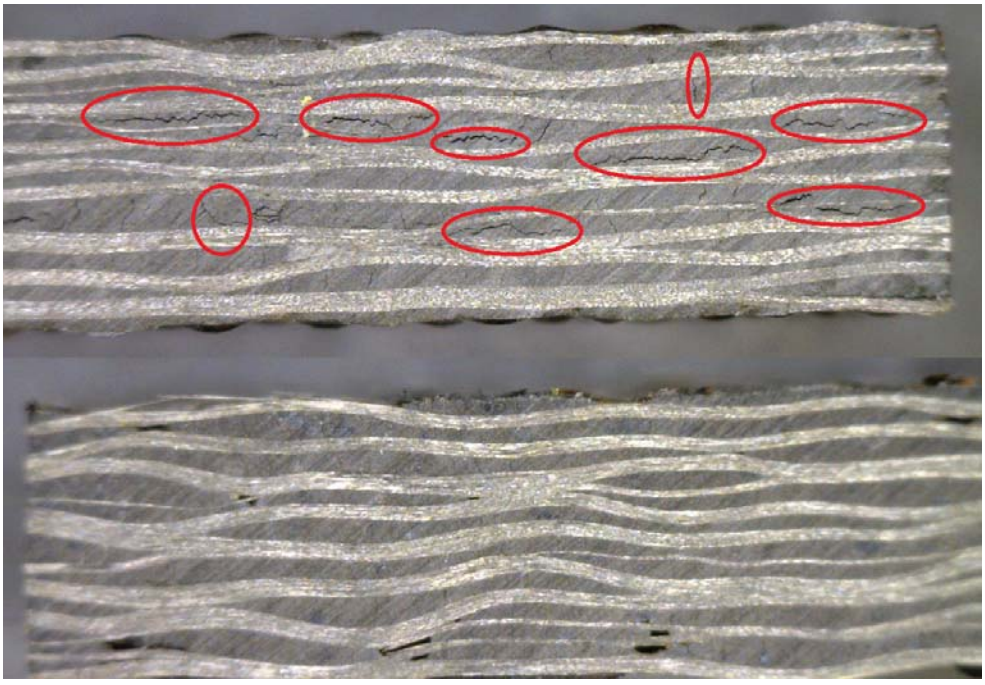

Figure 35. Post-TOS optical micrographs for PMR-15/IM7-4HSW-GP (upper) and 0N/ IM7-4HSW-GP (lower) composite cross-sections after 625 hours at 316 °C. The PMR-15 composite has grown microcracks while that from 0N has not.

Conclusions and Implications for Future Research

The viability of co-oligomerization of a POSS dianiline monomer designed to be highly thermally stable was successfully proven in SERDP project WP-2403. This monomer is suspected of being non-toxic and readily passed through the human body if inhaled/ingested due to its molecular architecture, but was not tested for in this effort. The POSS monomer was shown to be more thermally stable than MDA. Co-oligomerization was found to significantly improve processability marked by viscosity to the extent that it is an excellent candidate for consideration in the design of thermosetting systems for resin transfer molding. Composite laminates were fabricated with a POSS-containing oligomer without the use of solvent or need for pre-pregging. However, due to its volumetric molecular footprint, it increases network free volume to the extent that cured network glass transition temperature is significantly reduced. In attempts to mitigate this effect, crosslink density was increased to the extent that the resin suffered embrittlement, and the nadic crosslink concentration diminished thermal stability as this is the weak link in the network. Although all results indicate that network free volume is increased when POSS is incorporated into the architecture, a substantial decrease in moisture uptake was observed in comparison with other commercial polyimide systems, reducing the risk of composite structure failure due to rapid moisture release and knockdowns in mechanical and viscoelastic properties.

The POSS cage disappointedly did not exhibit signs of disassociating to form protective SiO_2 during long-term thermo-oxidative stability experiments, as seen when in the presence of atomic oxygen in low earth orbit (currently fielded in satellite protection systems to resist atomic oxygen). Development of a POSS segment that could perform this function at the operating temperatures of polyimide-based composites would represent a significant breakthrough. The POSS cage utilized in this study is too stable to disassociate between 300-400 °C, however, perhaps a cage with bond strain or a strategically chosen species inserted into its framework could facilitate cage opening and reaction with oxygen to form a regenerative SiO_2 layer that could provide protection to underlying composite from further oxidative attack.

The 0N POSS oligoimide, chosen for scaleup in this program, was found to suffer from the limitation of poor long-term TOS due to its high concentration of nadic end-cap. Research has been conducted by AFRL recently to examine the properties of analogous molecules with phenylethynyl end groups in one case, and in another with phenylethynyl end groups but the imide linkages removed. Both of these molecules exhibit similar traits to 0N, except they are much more thermally stable when cured, thus this problem has been overcome.

The most significant finding in this program was the elimination of micro-cracking concomitant with thermally induced oxidative degradation, as exhibited by the 0N-based composite. Recent discussions with industry regarding this finding have framed the magnitude of this shortcoming with organic matrix composite materials. This form of aging often precludes the use of these materials in applications where “light-weighting” would be of tremendous system benefit. Researchers have been trying to understand and solve this issue for decades to little avail. The key question that now needs to be answered is how much (or how little) POSS is actually required to eliminate micro-cracking? 0N is 80% by weight POSS and exhibited no micro-cracking after 625 hours at the upper long-term service temperature for PMR-15. Whether this resin can be simply used as a drop-in additive for commercial polyimide resin systems is an area of investigation that requires attention. Use of this class of materials to enhance processability and aging resistance has gained the attention of our industry, and we are aware of two companies investing albeit limited IR&D funds to further explore this technology.

Literature Cited

1. T.T. Serafini, P. Delvigs, G.R. Lightseg, J Appl Polym Sci, 1972, 16, 905.

2. P.J. Cavano, W.E. Winters, "PMR Polyimide/Graphite Fiber Composite Fan Blades," NASA CR-135113, pp. 5-6, December 1976.

3. P. Delvigs, W.B. Alston, R.D. Vannucci, "Effects of Graphite Fiber Stability on the Properties of PMR Polyimide Composites," NASA TM-79062, AVRADCOM TR 78-62, May 1979.

4. W.B. Alston, "Resin/Fiber Thermo-Oxidative Interactions in PMR Polyimide/Graphite Composites," NASA TM-79093, AVRADCOM TR 79-6, May 1979.

5. Calculated from www.denix.osd.mil/awards/upload/EEWSA-NAVAIR-NARRATIVE.pdf

6. F. P. Guengerich, J Biochem Mol Toxic, 2007, 21, 163-168.

7. F. P. Guengerich, Chem Res Toxicol, 2008, 21, 70-83.

8. C. H. Yun, T. Shimada and F. P. Guengerich, Carcinogenesis, 1992, 13, 217-222.

9. A. G. Siraki, T. S. Chan, G. Galati, S. Teng and P. J. O'Brien, Drug Metab Rev, 2002, 34, 549-564.

10. R. W. Scholz, K. S. Graham, E. Gumpricht and C. C. Reddy, Ann Ny Acad Sci, 1989, 570, 514-517.

11. R. E. Hughes, Nature, 1964, 203, 1068.

12. H. Kopelman, M. H. Robertson, P. G. Sanders and I. Ash, Br Med J, 1966, 1, 514-516.

13. Chuang, K. "High Tg Polyimides", NASA Tech Report 563972, 2002.

14. V. Vij, T. S. Haddad, G. R. Yandek, S. M. Ramirez, J. M. Mabry, "Synthesis of Polyhedral Oligomeric Silsesquioxane (POSS) Dianilines for use in High-Temperature Polyimides", Silicon, 2012, 4, 267.

15. C. McCusker, J. B. Carroll, V. M. Rotello, Chem. Comm. 2005, 996-998.

16. S. Skaria, S. Schriker, ACS Polymer Preprints 2005, 46(1), 94.

17. R. Y. Kannan, H. J. Salacinski, P. E. Butler, A. M. Seifalian, Acc. Chem. Res. 2005, 38, 879-884.

18. R. Y. Kannan, H. J. Salacinski, J. De Groot, I. Clatworthy, L. Bozec, M. Horton, E. Butler, A. M. Seifalian, Biomacromolecules 2006, 7, 215-223.

19. R. Y. Kannan, H. J. Salacinski, M. Odlyha, P. E. Butler, A. M. Seifalian, Biomaterials 2006, 27, 1971-1979.

20. G. Punshon, D. S. Vara, K. M. Sales, A. G. Kidane, H. J. Salacinski, A. M. Seifalian, Biomaterials 2005, 26, 6271-6279.

21. http://www.dailymail.co.uk/sciencetech/article-2266689/Cancer-victim-growing-new-nose-arm-Businessman-lost-organ-disease-hopes-new-sewn-face.html

22. D. M. Pinson, G. R. Yandek, T. S. Haddad, E. M. Horstman, J. M. Mabry, Macromolecules 2013. 46 (18), pp 7363-7377.

23. S. J. Tomczak, M. E. Wright, A. J. Guenthner, B. J. Petteys, T. K. Minton, A. Brunsvold, V. Vij, L. M. McGrath, J. M. Mabry, Polyimides and Other High Temperature Polymers 2009, 5, 227-245.

24. D. C. Malarik, R. D. Vannucci, NASA Technical Memorandum 105364, December, 1991.

25. J. K. Sutter, J. M. Jobe, E. A. Crane, J. Appl. Polym. Sci. 1995, 57, 1491-1499.

26. M. A. B. Meador, J. C. Johnston, Macromolecules 1997, 30, 3215-3223.

27. S. Wu, T. Hayakawa, R. Kikuchi, S. J. Grunzinger, M.-A. Kakimoto, H. Oikawa, Macromolecules 2007, 40(16), 5698-5705.

28. G. Mensitieri, M. Lavorgna, D. Larobina, G. Scherillo, G. Ragosta, P. Musto, Macromolecules 2008, 41, 4850-55.

29. J. D. Russell, J. L. Kardos, Polym. Comp. 1997, 18, 64.

30. Xuezhong By Zhang, Yudong Huang, Tianyu Wang, Lijiang Hu, Journal of Materials Science 2007, 42(13), 5264-5271.

Appendix

PAPERS AND PRESENTATIONS (APPROVED FOR PUBLIC RELEASE ONLY)

Lamb, Jason T.; Yandek, Gregory R.; Haddad, Timothy S.; Fernandes, Diane; Ford, Michael D.; Mabry, Joseph M. Reduced Micro-cracking in PMR-15 Type Resin Modified with Silsesquioxane Diamine Monomer; Manuscript submitted to Journal of Applied Polymer Science, Nov 2017.

Haddad, Tim S.; Yandek, Gregory R.; Zavala, Jacob; Lamb, Jason; Reams, Josiah; Ghiassi, Kamran; Mabry, Joseph M.; Guenthner, Andrew J. Silsesquioxane-Based Thermosetting Phenylethynyls: Synthesis, Thermally Induced Crosslinking and Thermophysical Properties; Abstracts of Papers, 253rd ACS National Meeting & Exposition, San Francisco, CA, United States, April 2-6, 2017 (2017), POLY-543.

Lamb, Jason T.; Yandek, Gregory R.; La Scala, John J.; Harvey, Benjamin G.; Palmese, Giuseppe R.; Eck, William S.; Sadler, Joshua M.; Yadav, Santosh K. Balancing Performance and Sustainability in Next-Generation PMR Technologies for OMC Structures; Featured Speaker at SAMPE Long Beach, May 26, 2016.

Haddad, Tim S.; Yandek, Gregory R.; Lamb, Jason; Ford, Michael D.; Mabry, Joseph M. Silsesquioxane-Based Thermosetting Oligoimides: Chemistry and Delivered Properties; From Abstracts of Papers, 250th ACS National Meeting & Exposition, Boston, MA, United States, August 16-20, 2015 (2015), POLY-79.

Lamb, Jason. Silsesquioxane-Based Aminated Monomers As Building Blocks in Thermosetting Oligoimides: Chemistry and Delivered Properties; From Abstracts of Papers, 250th ACS National Meeting & Exposition, Boston, MA, United States, August 16-20, 2015 (2015), POLY-351.

This Page Intentionally Left Blank

AFRL-RQ-ED-TR-2017-0025
Primary Distribution of this Report:

RQR
AFRL R&D Case Files
Completed Interim and Final Tech Reports Repository

AFRL/RQ Technical Library (2 CD + 1 HC)
6 Draco Drive
Edwards AFB, CA 93524-7130

Johns Hopkins University
Whiting School of Engineering
ATTN: Mary T. Gannaway/FSO
10630 Little Patuxent Pkwy, Suite 202
Columbia, MD 21044-3286

Defense Technical Information Center
(1 Electronic Submission via STINT)
Attn: DTIC-ACQS
8725 John J. Kingman Road, Suite 94
Ft. Belvoir, VA 22060-6218